

UMN-TH-2222/03
 FTPI-MINN-03/34
 DAMTP-2003-126
 UVIC-TH-03/09
 DESY 03-187
 hep-ph/0311314
 November 2003

Electric Dipole Moments in the MSSM at Large $\tan \beta$

Durmus Demir^(a), Oleg Lebedev^(b), Keith A. Olive^(a), Maxim Pospelov^(c,d) and Adam Ritz^(e)

^(a) *Theoretical Physics Institute, School of Physics and Astronomy,
 University of Minnesota, Minneapolis, MN 55455, USA*

^(b) *DESY Theory Group, D-22603 Hamburg, Germany*

^(c) *Centre for Theoretical Physics, CPES, University of Sussex, Brighton BN1 9QJ, UK*

^(d) *Department of Physics and Astronomy, University of Victoria,
 Victoria, BC, V8P 1A1 Canada*

^(e) *Department of Applied Mathematics and Theoretical Physics,
 Centre for Mathematical Sciences,
 University of Cambridge, Wilberforce Rd., Cambridge CB3 0WA, UK*

Abstract

Within the minimal supersymmetric standard model (MSSM), the large $\tan \beta$ regime can lead to important modifications in the pattern of CP-violating sources contributing to low energy electric dipole moments (EDMs). In particular, four-fermion CP-violating interactions induced by Higgs exchange should be accounted for alongside the constituent EDMs of quarks and electrons. To this end, we present a comprehensive analysis of three low energy EDM observables – namely the EDMs of thallium, mercury and the neutron – at large $\tan \beta$, in terms of one- and two-loop contributions to the constituent EDMs and four-fermion interactions. We concentrate on the constrained MSSM as well as the MSSM with non-universal Higgs masses, and include the CP-violating phases of μ and A . Our results indicate that the atomic EDMs receive significant corrections from four-fermion operators, especially when $\text{Im}(A)$ is the only CP-violating source, whereas the neutron EDM remains relatively insensitive to these effects. As a consequence, in a large portion of the parameter space, one cannot infer a separate bound on the electron EDM via the experimental constraint on the thallium EDM. Furthermore, we find that the electron EDM can be greatly reduced due to the destructive interference of one- and two-loop contributions with the latter being dominated by virtual staus.

1 Introduction

Electric dipole moments (EDMs) of the neutron [1] and heavy atoms and molecules [2, 3, 4, 5, 6, 7, 8] are primary observables in testing for flavor-neutral CP violation. The high degree of precision with which various experiments put limits on possible EDMs translates into stringent constraints on a variety of extensions of the Standard Model at and above the electroweak scale (see, e.g. [9]). The experiments that currently champion the best bounds on CP-violating parameters are the atomic EDMs of thallium and mercury and that of the neutron:

$$\begin{aligned} |d_{\text{Ti}}| &< 9 \times 10^{-25} e \text{ cm} \\ |d_{\text{Hg}}| &< 2 \times 10^{-28} e \text{ cm} \\ |d_n| &< 6 \times 10^{-26} e \text{ cm}. \end{aligned} \tag{1.1}$$

In this paper we address the theory of electric dipole moments in supersymmetric (SUSY) models with a large ratio of Higgs vacuum expectation values, or $\tan \beta$. Models with large $\tan \beta$ have recently received significant attention, stimulated in part by the final LEP results that impose significant constraints on the Higgs sector of the MSSM and imply a relatively large $\tan \beta$, $\tan \beta \gtrsim 5$ [10]. Another motivation for large $\tan \beta$ stems from unified theories, which allow for the unification of top and bottom Yukawa couplings when $\tan \beta \sim 50$ [11].

Supersymmetric models with the minimal field content (MSSM) allow for the presence of several CP-violating phases even in the most restrictive ansatz of flavor universality in the squark and slepton sectors. The null experimental EDM results pose a serious problem for the MSSM with superpartner masses around the electroweak scale. Indeed, a typical CP-violating SUSY phase of order one combined with $\mathcal{O}(100 \text{ GeV} - 1 \text{ TeV})$ masses for superpartners would violate experimental constraints by up to three orders of magnitude [12]. This generally requires the CP-violating phases to be very small, unless there are cancellations among different contributions [13, 14, 15] but these are largely disfavored by the mercury EDM constraint [16, 17, 18]. In string models, there are further complications since large EDMs are generally induced even if the SUSY breaking dynamics conserve CP (in the sense that the SUSY breaking F-terms are all real) [19]. Suppression of these unwanted effects requires rather special circumstances, e.g. dilaton domination with an approximate axial symmetry [20]. Other options to avoid overproduction of EDMs in SUSY models include heavy sfermions [21], the presence of extra dimensions [22], additional symmetries [23, 24], etc. Yet, despite the sizeable literature on EDMs in supersymmetric models, EDM constraints at large $\tan \beta$ remain poorly explored.

With this situation in mind, it is natural to ask what changes to the EDM predictions will occur at large $\tan \beta$? One simple observation is that the EDMs of the down quarks and the electrons, as induced by SUSY CP-violating phases, tend to grow because of their dependence on the down-type Yukawa couplings which translates into a linear enhancement in $\tan \beta$. The second and in some sense more profound change was for a long time overlooked in the SUSY-EDM literature. At large $\tan \beta$, the observable EDMs of neutrons and heavy

atoms receive contributions not only from the EDMs of the constituent particles, such as electrons and quarks, but also from CP-odd *four-fermion operators*. The latter operators, since they are induced by Higgs exchange, receive an even more significant enhancement by several powers of $\tan \beta$. The necessity of including these operators in the EDM analysis was shown by Barr [25] for the case of a two Higgs doublet model with spontaneous breaking of CP, and recently by Lebedev and Pospelov [26] for the MSSM with explicit CP violation.

In this paper, we present a thorough analysis of EDMs in the large $\tan \beta$ regime. We analyze the predictions for the three observables that champion the best constraints on the CP-odd sector of the theory: the atomic EDMs of thallium and mercury [2, 3], and the neutron EDM [1]. The restrictive assumption of Ref. [26] on the parametrically large superpartner mass scale will be lifted in this paper, and the effects of the four-fermion operators are analyzed alongside the usual electron and quark EDM and color EDM (CEDM) contributions. We first consider a framework in which the scalar and gaugino masses, m_0 and $m_{1/2}$, as well as the tri-linear terms A_0 , are unified at the GUT scale, i.e. the constrained MSSM (CMSSM) [27, 28]. In the CMSSM, the Higgs mixing mass, μ , and the pseudoscalar Higgs mass, m_A , are determined by the GUT scale parameters, $m_{1/2}, m_0, A_0$, and $\tan \beta$ using the radiative electroweak symmetry conditions. The sign of μ is also free in the CP-conserving version of the CMSSM. We then repeat the same analysis for the case when scalar universality is relaxed in the Higgs sector (NUHM) [29, 30]. In this case, the Higgs soft masses m_1 and m_2 can be chosen independently of the squark and slepton masses, which remain unified at the GUT scale. Alternatively, one may choose μ and m_A as free parameters and use the RGEs to determine m_1 and m_2 at the GUT scale. The positivity of m_1^2 and m_2^2 at the GUT scale may impose a restriction on the parameter space in this case.

The universality of the gaugino masses at the GUT scale limits the number of physical SUSY CP-violating phases to two¹, which in the real gaugino mass basis can be identified with the phases of the μ and A parameters. We perform the analysis separately for these two phases, as the scaling of the EDMs with $\tan \beta$ is quite different in each case.

The paper is organized as follows. In the next section we review the structure of the effective CP-odd Lagrangian at 1 GeV. We argue that at large $\tan \beta$ it should be modified by the presence of four-fermion operators. We then estimate the SUSY parameter regimes where these contributions become important sources for EDMs. Section 3 calculates the supersymmetric threshold corrections that induce CP violation via Higgs exchange. Section 4 addresses the modifications of the thallium, mercury and neutron EDMs due to the presence of four-fermion operators and provides general formulae for these observables. In section 5 we perform a numerical analysis of EDMs at $\tan \beta = 50$ in the CMSSM and the NUHM. Section 6 concludes the paper by summarizing the modifications to the EDM bounds at large $\tan \beta$ and discussing the importance of different contributions to the EDMs.

¹This is a consequence of the $U(1)_R$ and Peccei–Quinn symmetries which allow us to eliminate two CP-violating phases (those of $B\mu$ and gaugino masses). In the flavor–nonuniversal case, some of the phases can also be rotated away by redefining the quark superfields, such that the physical SUSY CP-violating phases are reparametrization invariant combinations of the SUSY and SM flavor structures [31].

Some additional details on relevant hadronic calculations are given in appendices A and B.

2 The structure of the low energy Lagrangian

We begin by recalling the standard structure of the effective CP-odd Lagrangian normalized at 1 GeV, which is the lowest scale allowing for a perturbative quark-gluon description. It includes the theta term, the Weinberg operator, the EDMs of quarks and electrons, and the color EDMs of quarks:

$$\begin{aligned} \mathcal{L}_{eff} = & \frac{g_s^2}{32\pi^2} \bar{\theta} G_{\mu\nu}^a \tilde{G}^{\mu\nu,a} + \frac{1}{3} w f^{abc} G_{\mu\nu}^a \tilde{G}^{\nu\beta,b} G_{\beta}^{\mu,c} \\ & - \frac{i}{2} \sum_{i=e,u,d,s} d_i \bar{\psi}_i (F\sigma) \gamma_5 \psi - \frac{i}{2} \sum_{i=u,d,s} \tilde{d}_i \bar{\psi}_i g_s (G\sigma) \gamma_5 \psi + \dots \end{aligned} \quad (2.2)$$

For a given pattern of supersymmetry breaking d_i , \tilde{d}_i , and w can be calculated explicitly, via one or two-loop SUSY diagrams, and evolved down to 1 GeV using perturbative QCD. On the other hand, only the additive radiative corrections to the theta term can be calculated, leaving $\bar{\theta}$ as a free parameter subject to an arbitrary initial condition. In supersymmetric models with CP-violating phases larger than $\sim 10^{-8}$ in the flavor-diagonal sector the only reasonable strategy to avoid the strong CP problem is to postulate the existence of the Peccei-Quinn relaxation mechanism [32], which removes the theta term from the list of contributing operators. We will therefore adopt this strategy and discard $\bar{\theta}$. When $\tan\beta$ is low, possible four fermion CP-odd operators (e.g. $(\bar{q}q)(\bar{q}i\gamma_5 q)$ and alike) can be safely neglected. Indeed, these operators involve a double flip of helicity associated with an additional $(m_q/v_{EW})^2$ suppression, and this makes these operators effectively of dimension 8, and thus totally negligible.

The dependence of the experimentally measured EDMs of neutrons, and paramagnetic and diamagnetic atoms, on the Wilson coefficients in (2.2), as calculated at low $\tan\beta$, can be symbolically presented in the following way:

$$\begin{aligned} d_{Tl} &= d_{Tl}(d_e) \\ d_n &= d_n(\bar{\theta}, d_i, \tilde{d}_i, w) \quad \text{at low } \tan\beta. \\ d_{Hg} &= d_{Hg}(\bar{\theta}, \tilde{d}_i, d_i, w) \end{aligned} \quad (2.3)$$

The dependence of the EDMs of paramagnetic atoms and molecules (such as thallium) on the electron EDM alone makes them the most valuable observables for SUSY models, as they allow us to link the experimental results directly to a calculable combination of CP-violating phases, and slepton and gaugino masses, while the uncertainty of atomic calculations enters as an overall factor. In fact, due to this property of paramagnetic EDMs, it is customary to quote the limit on d_e directly, skipping the actual experimental limit on the EDM of the paramagnetic atom. The EDMs of the neutron and mercury are far more complicated as a variety of hadronic (and in the case of mercury also nuclear and

atomic) matrix elements are needed in order translate the experimental results into limits on a specific combination of the Wilson coefficients.

The structure of the effective Lagrangian becomes even more complicated if $\tan\beta$ is taken to be a large parameter. Indeed, the operators induced by Higgs exchange that involve down-type quarks and charged leptons grow rapidly with $\tan\beta$ [26]. For now, we parametrize these operators by coefficients C_{ij} ,

$$\mathcal{L}_{eff}^{4f} = \sum_{i,j=e,d,s,b} C_{ij} (\bar{\psi}_i \psi_i) (\bar{\psi}_j i \gamma_5 \psi_j), \quad (2.4)$$

where i, j run over flavor indices and the second index always indicates the fermion flavor that enters (2.4) via a pseudoscalar bilinear. These operators represent a subclass of the larger set of all possible CP-odd flavor-conserving four-fermion operators considered in [33, 34, 35]. Note that the b -quark is heavy compared to the scale of 1 GeV and thus can be integrated out, producing new dimension 7 operators $\bar{\psi}_i \psi_i (G_{\mu\nu}^a \tilde{G}^{\mu\nu,a})$ and $\bar{\psi}_i i \gamma_5 \psi_i (G_{\mu\nu}^a G^{\mu\nu,a})$ and leading to new higher loop contributions to d_i , \tilde{d}_i and w . With this procedure in mind, we prefer to keep the coefficients C_{bi} and C_{ib} explicitly so that integrating out the b -quarks is interpreted as part of taking the corresponding matrix element.

When the contributions from C_{ij} are not negligible, the relation between the observables and the SUSY parameters encoded in the Wilson coefficients of Eqs. (2.2) and (2.4) becomes considerably more involved:

$$\begin{aligned} d_{\text{TI}} &= d_{\text{TI}}(d_e, C_{de}, C_{se}, C_{be}) \\ d_n &= d_n(\bar{\theta}, d_i, \tilde{d}_i, w, C_{q_1 q_2}) \quad \text{at large } \tan\beta. \\ d_{\text{Hg}} &= d_{\text{Hg}}(\bar{\theta}, d_i, \tilde{d}_i, w, C_{ij}). \end{aligned} \quad (2.5)$$

Paramagnetic EDMs lose their one-to-one relation to d_e , as they also become dependent on operators that involve quarks and gluons, and as a consequence are subject to considerable hadronic uncertainties. Hence, at large $\tan\beta$, a separate bound on d_e simply may not exist, and the bound on the EDM of the paramagnetic atom (molecule) as a whole should be used instead. The mercury EDM receives a number of additional contributions from semileptonic and pure hadronic four-fermion operators. As a consequence, $(\tilde{d}_u - \tilde{d}_d)$ may no longer be the dominant contribution to d_{Hg} in contrast to the situation at low $\tan\beta$ [16]. Thus, the large $\tan\beta$ regime is qualitatively different from $\tan\beta \sim \mathcal{O}(1)$ and requires a separate dedicated analysis.

To conclude this section, we will determine a combination of SUSY parameters that regulates which effect is more important: one-loop EDMs or four-fermion operators. The required interpolating parameter can be deduced from the asymptotics of the one-loop EDMs and four-fermion operators in the limit of a generic heavy superpartner mass scale M . For simplicity, and in this section only, we will not differentiate among different superpartners and assume the same mass for squarks, sleptons, gauginos, etc.

Let us first consider a non-zero μ -phase (relative to the gaugino mass). While the one-loop EDMs generally scale as $d_i/m_i \sim \mu m_\lambda \tan\beta \sin\theta_\mu/M^4$, the leading order contributions

to C_{ij} scale as $C \sim \mu m_\lambda (\tan \beta)^3 \sin \theta_\mu / (M^2 m_A^2)$ [26], where θ_μ is the CP-violating phase, m_λ is a gaugino mass, and $M = \max(m_0, m_{1/2})$ stands for a sfermion or gaugino mass, whichever is larger. Thus, we can introduce the following combination of SUSY parameters that interpolates between the two regimes:

$$\xi \equiv \frac{M}{m_A} \tan \beta. \quad (2.6)$$

In the limit of large M , with m_A fixed at the electroweak scale, all EDM-like observables are dominated by the four-fermion operators [26]. When M is kept finite, there is a certain critical value for ξ below which the usual one-loop EDMs dominate the observables, and above which the four-fermion operators are more important.

Using the results of Refs. [26, 16], we can estimate the critical value for ξ in the limit when all superpartner masses are approximated by some heavy scale $m_0 \sim m_{1/2} \sim M \gtrsim v_{EW} \sim 246$ GeV, while m_A is kept fixed near the electroweak scale. If all CP violation is induced by θ_μ , the relative importance of the two sources is determined by the ratio

$$\frac{d_{\text{TI}}(C_{ij})}{d_{\text{TI}}(d_e)} \simeq 10^{-5} \left[\frac{M}{m_A} \tan \beta \right]^2 = 10^{-5} \xi^2, \quad (2.7)$$

which suggests a critical value for ξ ,

$$\xi_c \sim 300 \quad \text{for} \quad \theta_\mu \neq 0. \quad (2.8)$$

From this estimate it becomes clear that when $m_A \simeq M$ the effects of the four-fermion operators are subleading but not negligible, reaching 20% of the d_e contribution at maximal $\tan \beta$. On the other hand, even a mild hierarchy between the mass scales, $M \gtrsim 5m_A$, may lead to a contribution to atomic EDMs comparable to d_e , or even to dominance of the four-fermion contributions.

In the case of the other CP-violating phase θ_A , the relative phase of the A parameter and the gaugino mass, we estimate that the transition to dominance of the four-fermion operators takes place at

$$\xi_c \tan^{1/2} \beta \sim 500 \quad \text{for} \quad \theta_A \neq 0. \quad (2.9)$$

Here, the additional power of $\tan \beta$ arises from the fact that the one-loop induced $d_e(\theta_A)$ does not grow with $\tan \beta$. Thus in this case, even for $m_A \sim M$, the contribution of the four-fermion operators may become comparable to d_e .

Both conditions (2.8) and (2.9) can be realized in a generic SUSY spectrum, but how realistic are they for the constrained MSSM and the MSSM with non-universal Higgs masses? We note that the simple comparison of d_e and C_{ij} made in this section may be subject to significant modifications, as the masses of sleptons and squarks as well as other superpartners are affected by the renormalization group evolution from the GUT scale to the electroweak scale. Therefore, we now turn to a numerical comparison of all contributions to the EDMs for different CP-violating phases and different patterns of SUSY breaking at large $\tan \beta$, as detailed in the next four sections.

3 CP-odd four-fermion operators in the MSSM

We now turn to specific SUSY mechanisms that generate C_{ij} . As shown in Ref. [26], C_{ij} are generated primarily through the exchange of the pseudoscalar and scalar Higgs particles A and H with CP violation entering through vertex corrections. This dominates the one-loop induced C_{ij} due to large $\mathcal{O}(\tan^3 \beta)$ enhancements. Other contributions, such as CP-odd higher-loop effects, SUSY box diagrams, etc., can have an even stronger dependence on $\tan \beta$. However, these effects are further suppressed either by additional loop factors or by additional powers of small Yukawa couplings and in this sense are subleading. Nevertheless, $A - H$ mixing may be numerically important [26], and therefore its contribution has to be included in the EDM analysis.

3.1 Higgs-mediated CP-odd four-fermion operators

The $\tan \beta$ enhancement of certain loop corrections in the down-type quark and charged lepton sectors is a well studied phenomenon [36]. Supersymmetric threshold corrections, such as those in Fig. 1, generate a new Yukawa interaction which is absent in the limit of exact supersymmetry. As a result, below the superpartner scale, the Yukawa interactions in the D -quark and charged lepton sectors are given by

$$\begin{aligned} -\mathcal{L}_Y = & (Y_D^{(0)} + Y_D^{(1)}) H_1 D_R^\dagger D_L + \mathcal{Y}_D H_2^\dagger D_R^\dagger D_L \\ & + (Y_E^{(0)} + Y_E^{(1)}) H_1 E_R^\dagger E_L + \mathcal{Y}_E H_2^\dagger E_R^\dagger E_L + \text{h.c.} , \end{aligned} \quad (3.10)$$

where $Y_{D,E}^{(0)}$ are the tree level Yukawa couplings and $\mathcal{Y}_{D,E}$ and $Y_{D,E}^{(1)}$ are the one-loop-induced couplings. Thus, instead of being the Yukawa sector of a type II two-Higgs doublet model, Eq. (3.10) represents a generic two Higgs doublet model where Higgs exchange may lead to violation of CP. One should keep in mind that Eq. (3.10) is valid in the limit of heavy superpartners. If the scale of SUSY breaking is close to the electroweak scale one should also include additional radiatively generated operators, e.g. $(H_2^\dagger H_2)^n H_2^\dagger D_R^\dagger D_L$.

Due to flavor universality in the soft-breaking sector, flavor-changing effects can be ignored in EDM calculations, and a simple linear relation between $Y_{D,E}^{(0)}$ and $\mathcal{Y}_{D,E}$ holds for every D and E flavor:

$$\mathcal{Y}_D = J_D Y_D^{(0)}, \quad \mathcal{Y}_E = J_E Y_E^{(0)}. \quad (3.11)$$

The calculation of the loop functions J_D and J_E is straightforward but tedious, as a large number of SUSY diagrams contribute. Nevertheless, an analytical result for this set of loop diagrams is possible, and we present it in the next subsection.

SUSY CP violation arises from a mismatch between the phases of the μ and A parameters, and $m_{1/2}$, and leads to complex masses and Yukawa couplings. The quark and lepton masses,

$$\begin{aligned} -\mathcal{L}_{\text{mass}} = & (Y_D^{(0)} + Y_D^{(1)}) \langle H_1 \rangle D_R^\dagger D_L + \mathcal{Y}_D \langle H_2 \rangle D_R^\dagger D_L \\ & + (Y_E^{(0)} + Y_E^{(1)}) \langle H_1 \rangle E_R^\dagger E_L + \mathcal{Y}_E \langle H_2 \rangle E_R^\dagger E_L + \text{h.c.} , \end{aligned} \quad (3.12)$$

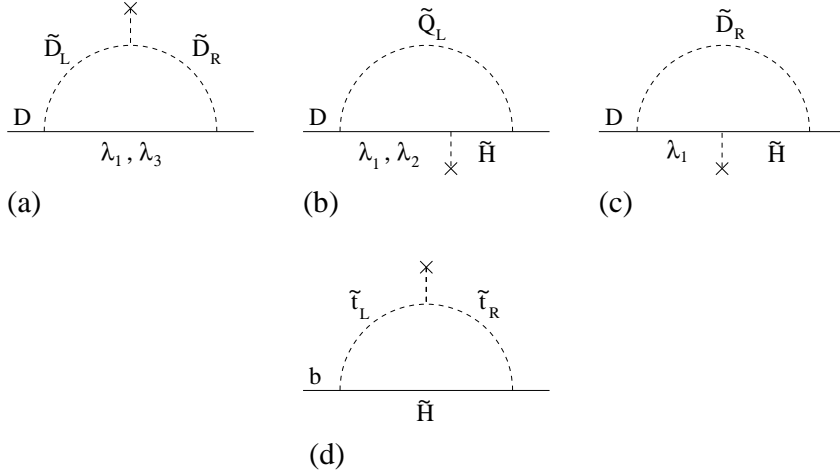


Figure 1: One-loop SUSY threshold corrections in the down quark and charged lepton Yukawa sectors. All four types of diagrams are relevant for the b -quark, while only (a)-(c) contribute in the case of d and s quarks, and the electron. Here λ_i denote the gauginos. The vacuum insertion of $\langle H_2 \rangle$ indicated by a cross is for illustrative purposes only as all calculations are performed in the mass eigenstate basis.

can be made real via a chiral rotation of the D and E fields,

$$D_R \rightarrow e^{-i\delta_D^{(m)}} D_R, \quad E_R \rightarrow e^{-i\delta_E^{(m)}} E_R, \quad (3.13)$$

where the rotation angles are defined by $\tan \beta$ and the loop functions J_i :

$$\delta_i^{(m)} = \text{Arg}(Y_i^{(0)} + Y_i^{(1)} + \mathcal{Y}_i \tan \beta) \simeq \text{Arg}(Y_i^{(0)} + Y_i^{(1)}) + \text{Arg}(1 + J_i \tan \beta), \quad (3.14)$$

where $i = d, s, b, e$ are the flavors of interest. $Y_i^{(1)}$ contains a loop suppression factor and thus can be neglected. However, a large value of $\tan \beta$ can compensate the loop suppression of \mathcal{Y}_i so that the phases $\text{Arg}(1 + J_i \tan \beta)$ can be of order one. The vertices of the A and H Higgs bosons and fermions, as derived from the Lagrangian (3.10), also contain a complex phase:

$$\delta_i^{(H)} = \text{Arg}((Y_i^{(0)} + Y_i^{(1)}) \tan \beta + \mathcal{Y}_i) \simeq \text{Arg}(Y_i^{(0)} + Y_i^{(1)}). \quad (3.15)$$

This equation is written under the assumption that $\tan \beta$ is a large parameter. The difference between these two phases,

$$\delta_i = \delta_i^{(m)} - \delta_i^{(H)}, \quad (3.16)$$

constitutes a physical CP-violating phase that enters into the interactions of H and A with physical fermions ψ_i ,

$$\mathcal{L}_{\text{CPV}} = - \sum_{i=d,s,b,e} \frac{Y_i}{\sqrt{2}} \sin \delta_i (\bar{\psi}_i \psi_i A + \bar{\psi}_i i \gamma_5 \psi_i H). \quad (3.17)$$

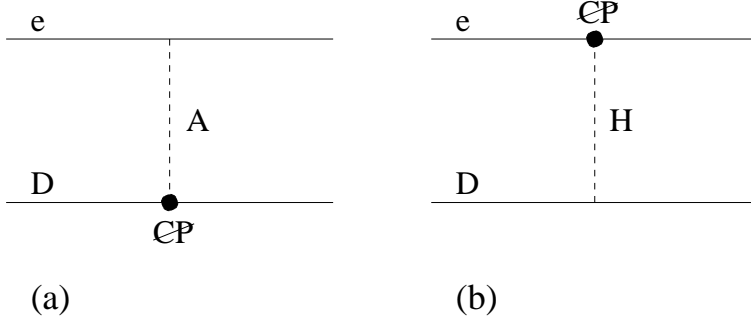


Figure 2: The Higgs-mediated electron-quark interaction C_{qe} with CP violation at the Higgs-quark vertex (a) and at the Higgs-electron vertex (b).

Note that the phase $\text{Arg}(Y_i^{(0)} + Y_i^{(1)})$ drops out of the expression for δ_i as it should. An exchange by the physical Higgses, as in Fig. 2, will then produce CP-odd four-fermion interactions with the following coefficients

$$C_{ij}^{(\text{vc})}(i, j = e, d, s, b) = -\frac{\tan^2 \beta}{2m_A^2} \frac{Y_i^{SM} Y_j^{SM} \sin(\delta_i - \delta_j)}{|1 + J_i \tan \beta| |1 + J_j \tan \beta|}. \quad (3.18)$$

Here Y_f^{SM} denote the Standard Model values for the Yukawa couplings, $Y_f^{SM} \equiv \sqrt{2}m_f/v$ ($v=246$ GeV), and the superscript of $C_{ij}^{(\text{vc})}$ signifies that this contribution originates from a vertex correction. Note also that at leading order in $\tan \beta$ an exchange by the (lightest) h -Higgs does not contribute to C_{ij} , the difference between m_A and m_H can be ignored, and the neutral Higgs mixing angle is trivial, $\cos^2 \alpha \simeq 1$.

Examining expression (3.18), we notice immediately that

$$C_{ij}^{(\text{vc})} = -C_{ji}^{(\text{vc})}, \quad (3.19)$$

and thus vertex corrections do not generate four-fermion operators that involve a single flavor such as, for example, $\bar{d}d\bar{i}\gamma_5 d$.

Combining Eqs. (3.14) and (3.18), we observe that the coefficients C_{ij} grow as $\mathcal{O}(\tan^3 \beta)$ as long as $J_{i(j)} \tan \beta < 1$, which is true for almost the entire available domain of $\tan \beta$. Moreover, the cubic growth of C_{ij} generated at one loop due to explicit CP violation in the soft breaking sector is distinct from the $\mathcal{O}(\tan^2 \beta)$ -behavior of C_{ij} in two-Higgs doublet models with spontaneous CP violation [25].

3.1.1 Beyond the limit of heavy superpartners

In order to go beyond the approximation of heavy superpartners, one should reformulate Eq. (3.18) in terms of the tree-level fermion masses $m_i^{(0)} = Y_i^{(0)}v_1/\sqrt{2}$ and the one-loop SUSY corrections to the fermion masses Δm_i , where *all operators* neglected in Eq. (3.10)

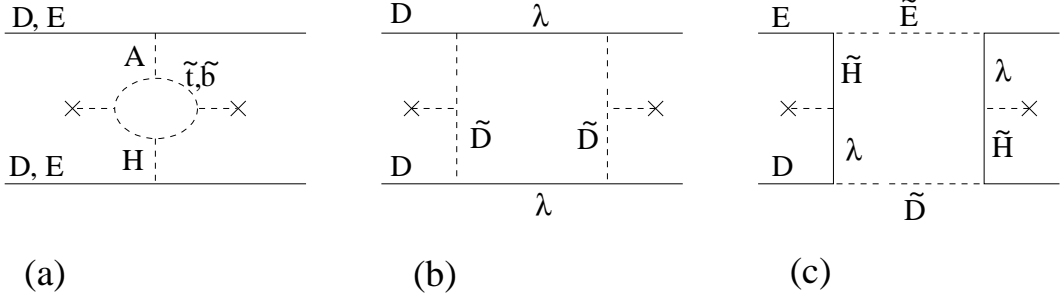


Figure 3: Diagrams that generate subleading contributions to C_{ij} . (a) is the radiatively generated $H - A$ mixing, and (b)-(c) are typical box diagrams.

are included². The one-loop-corrected mass terms can be made real by a phase redefinition (3.13) with the phase now given by

$$\delta_i^{(m)} = \text{Arg}(1 + \Delta m_i / m_i^{(0)}) . \quad (3.20)$$

Here we assume for convenience that $m_i^{(0)}$ is real. In the large $\tan \beta$ regime, the couplings of A and H Higgses to fermions can be obtained as a derivative of $m_i^{(0)} + \Delta m_i$ with respect to $\langle H_1 \rangle = v_1$ at $v_1 = 0$, and thus the phase $\delta_i^{(H)}$ is now given by

$$\delta_i^{(H)} = \text{Arg} \left(\frac{\partial(m_i^{(0)} + \Delta m_i)}{\partial v_1} \right) . \quad (3.21)$$

In the large $\tan \beta$ regime it is natural to expect that $\delta_i^{(H)} \ll \delta_i^{(m)}$, so that the physical CP-violating phase δ_i is given by $\text{Arg}(1 + \Delta m_i / m_i^{(0)})$. However, in practice it often happens that $\delta_i^{(H)}$ cannot be neglected (see Sec. 5.1). Finally, the coefficients $1 + J_i \tan \beta$ appearing in the denominator of Eq. (3.18) should also be replaced by the expression $1 + \Delta m_i / m_i^{(0)}$ (which is independent of $m_i^{(0)}$ because Δm_i is proportional to $m_i^{(0)}$). With these modifications, Eq.(3.18) takes the form

$$C_{ij}^{(\text{vc})}(i, j = e, d, s, b) = - \frac{\tan^2 \beta}{2m_A^2} \frac{Y_i^{SM} Y_j^{SM} \sin(\delta_i - \delta_j)}{|1 + \Delta m_i / m_i^{(0)}| |1 + \Delta m_j / m_j^{(0)}|} , \quad (3.22)$$

where the phases δ_i are given in the expressions (3.16), (3.20) and (3.21). Eq. (3.22) shows that the crucial step in calculating the CP-odd operators C_{ij} is finding the one-loop correction to the masses of the d, s, b quarks and the electron.

At subleading order in $\tan \beta$, there are a large number of diagrams that contribute to C_{ij} , examples of which are given in Fig. 3. The complete calculation of these diagrams goes beyond the scope of the present paper. However, as shown in Ref. [26], the CP-odd

²A more complete approach would necessitate the use of the Coleman–Weinberg effective potential. For our purposes, however, it suffices to truncate the series of non-renormalizable operators.

mixing of $H - A$ Higgs bosons may sometimes be numerically important and comparable to (3.22). However, since the $H - A$ mixing term contains either a loop factor which is not compensated by large $\tan \beta$ or a suppression by $(Y_{b(\tau)}^{SM})^2 \tan \beta$, $H - A$ mixing may only become significant with the help of an additional mass hierarchy. In particular, if the following combination is large [26, 37],

$$\frac{A^2 \mu^2 v^2}{m_{\text{squark}}^4 m_A^2} \gg 1, \quad (3.23)$$

$H - A$ mixing may provide a sizeable contribution to the EDMs. The box diagrams scale differently and lose their importance when the superpartners are heavy, $m_0 \sim m_{1/2} \gg v$. Since this is one of the most interesting domains of the parameter space, we include the effects of $H - A$ mixing and neglect the box diagrams.

The coefficients C_{ij} induced by diagrams 3a can be calculated with the use of the following formula:

$$C_{ij}^{(AH)} \simeq \frac{\langle AH \rangle \tan^2 \beta}{2m_A^4} \frac{Y_i^{SM} Y_j^{SM}}{|1 + \Delta m_i/m_i^{(0)}| |1 + \Delta m_j/m_j^{(0)}|}, \quad (3.24)$$

where $i, j = d, s, b, e$ and $\langle AH \rangle$ stands for the one-loop-generated amplitude in the effective Higgs Lagrangian,

$$\mathcal{L}_{H,A} = -\frac{1}{2}m_A^2 A^2 - \frac{1}{2}m_H^2 H^2 - \langle AH \rangle AH + \dots, \quad (3.25)$$

where the $\langle AH \rangle$ mixing parameter has the dimension of mass squared. Eq. (3.24) also uses $m_H^2 \simeq m_A^2 \gg \langle AH \rangle$ and $\tan \beta \gg 1$. The effect of $A - h$ mixing, where $h \sim \text{Re}(H_2 - \langle H_2 \rangle)$, is negligible under these conditions. In this approximation, it is not necessary to re-diagonalize the 3×3 Higgs mass matrix. It suffices to simply account for $\langle AH \rangle$ by a direct insertion on the Higgs line in Fig. 3a. Note that $C_{ij}^{(AH)}$ are flavor-symmetric,

$$C_{ij}^{(AH)} = C_{ji}^{(AH)}, \quad (3.26)$$

and, unlike the vertex corrections, can generate a single flavor four-fermion operator.

3.2 SUSY threshold corrections in the mass sector and scalar-pseudoscalar mixing

In this subsection we provide a complete set of threshold corrections Δm_i , at leading order in $\tan \beta$, to the quark and lepton masses (ignoring flavor mixing). Let us first briefly summarize our notation which, unless noted below, follows that of Ref. [38]. The chargino and neutralino mass matrices are diagonalized by

$$\begin{aligned} U^* M_{\chi^+} V^\dagger &= \text{diag}(m_{\chi_1^+}, m_{\chi_2^+}), \\ N^* M_{\chi^0} N^\dagger &= \text{diag}(m_{\chi_1^0}, \dots, m_{\chi_4^0}), \end{aligned} \quad (3.27)$$

where U, V , and N are unitary matrices. In addition, the sfermion mass matrix is diagonalized by the matrix

$$\begin{pmatrix} c_f & s_f e^{i\phi_f} \\ -s_f e^{-i\phi_f} & c_f \end{pmatrix}, \quad (3.28)$$

that rotates the basis $(\tilde{f}_L, \tilde{f}_R)$ to the mass eigenstate basis $(\tilde{f}_1, \tilde{f}_2)$. Here $c_f \equiv \cos \theta_f$, $s_f \equiv \sin \theta_f$, and θ_f is the sfermion mixing angle (see [38] for the explicit form of the mass matrices). In our convention the CP-violating phase appearing in the sfermion mixing mass is given by³

$$\phi_f = \text{Arg} \left[-(A_f^* + \mu R_f) \right], \quad (3.29)$$

where $R_f = \tan \beta$ for $I_3 = -1/2$ and $R_f = \cot \beta$ for $I_3 = 1/2$.

As argued in the previous section, a large value of $\tan \beta$ can compensate the loop suppression of Δm_i such that the consequent CP-violating phase is of order one. Below we list the relevant supersymmetric contributions to Δm_i which grow linearly with $\tan \beta$. We omit the superscript in $m_i^{(0)}$ for brevity.

(i) Corrections to the down-type quark masses

For all three down-type flavors, d , s and b (where m_3 and ϕ_3 denote the gluino mass and its phase, and $\alpha_w = g^2/4\pi$):

$$\begin{aligned} (\Delta m_d)_{\lambda_3} &= \frac{2\alpha_s}{3\pi} e^{-i(\phi_d + \phi_3)} s_d c_d m_3 (m_{\tilde{d}_1}^2 - m_{\tilde{d}_2}^2) I(m_{\tilde{d}_1}^2, m_{\tilde{d}_2}^2, m_3^2), \\ (\Delta m_d)_{\chi^+} &= -\frac{\alpha_w m_d}{4\sqrt{2}\pi m_w \cos \beta} \sum_i U_{i2}^* V_{i1}^* m_{\chi_i^+} \left[c_u^2 \tilde{B}_0(m_{\tilde{u}_1}^2, m_{\chi_i^+}^2) + s_u^2 \tilde{B}_0(m_{\tilde{u}_2}^2, m_{\chi_i^+}^2) \right], \\ (\Delta m_d)_{\chi^0} &= -\frac{\alpha_w}{36\pi} e^{-i\phi_d} \tan \theta_W s_d c_d (m_{\tilde{d}_1}^2 - m_{\tilde{d}_2}^2) \sum_i N_{i1}^* (N_{i1}^* \tan \theta_W - 3N_{i2}^*) m_{\chi_i^0} \\ &\quad \times I(m_{\tilde{d}_1}^2, m_{\tilde{d}_2}^2, m_{\chi_i^0}^2) \\ &+ \frac{\alpha_w m_d}{24\pi m_w \cos \beta} \sum_i N_{i3}^* (N_{i1}^* \tan \theta_W - 3N_{i2}^*) m_{\chi_i^0} \left[c_d^2 \tilde{B}_0(m_{\tilde{d}_1}^2, m_{\chi_i^0}^2) \right. \\ &+ \left. s_d^2 \tilde{B}_0(m_{\tilde{d}_2}^2, m_{\chi_i^0}^2) \right] \\ &- \frac{\alpha_w m_d}{12\pi m_w \cos \beta} \tan \theta_W \sum_i N_{i3}^* N_{i1}^* m_{\chi_i^0} \left[s_d^2 \tilde{B}_0(m_{\tilde{d}_1}^2, m_{\chi_i^0}^2) + c_d^2 \tilde{B}_0(m_{\tilde{d}_2}^2, m_{\chi_i^0}^2) \right]. \end{aligned} \quad (3.30)$$

In addition, for the b -quark there is a “pure higgsino” contribution:

$$\begin{aligned} (\Delta m_b)_{\chi^+} &= -\frac{\alpha_w m_t m_b}{8\pi m_w^2 \sin \beta \cos \beta} e^{i\phi_t} c_t s_t (m_{\tilde{t}_1}^2 - m_{\tilde{t}_2}^2) \sum_i U_{i2}^* V_{i2}^* m_{\chi_i^+} \\ &\quad \times I(m_{\tilde{t}_1}^2, m_{\tilde{t}_2}^2, m_{\chi_i^+}^2). \end{aligned} \quad (3.31)$$

³This convention for the phase of A corresponds to the following normalization of the left-right mixing terms in the squark mass matrix: $m_{LR}^2 = -m_f (A_f^* + \mu R_f)$.

(ii) Corrections to the charged lepton masses

$$(\Delta m_e)_{\chi^+} = -\frac{\alpha_w m_e}{4\sqrt{2}\pi m_w \cos \beta} \sum_i U_{i2}^* V_{i1}^* m_{\chi_i^+} \tilde{B}_0(m_{\tilde{\nu}_L}^2, m_{\chi_i^+}^2), \quad (3.32)$$

$$\begin{aligned} (\Delta m_e)_{\chi^0} &= \frac{\alpha_w}{4\pi} e^{-i\phi_e} \tan \theta_W s_e c_e (m_{\tilde{e}_1}^2 - m_{\tilde{e}_2}^2) \sum_i N_{i1}^* (N_{i2}^* + \tan \theta_W N_{i1}^*) m_{\chi_i^0} \\ &\quad \times I(m_{\tilde{e}_1}^2, m_{\tilde{e}_2}^2, m_{\chi_i^0}^2) \\ &- \frac{\alpha_w m_e}{8\pi m_w \cos \beta} \sum_i N_{i3}^* (N_{i1}^* \tan \theta_W + N_{i2}^*) m_{\chi_i^0} [c_e^2 \tilde{B}_0(m_{\tilde{e}_1}^2, m_{\chi_i^0}^2) \\ &+ s_e^2 \tilde{B}_0(m_{\tilde{e}_2}^2, m_{\chi_i^0}^2)] \\ &- \frac{\alpha_w m_e}{4\pi m_w \cos \beta} \tan \theta_W \sum_i N_{i3}^* N_{i1}^* m_{\chi_i^0} [s_e^2 \tilde{B}_0(m_{\tilde{e}_1}^2, m_{\chi_i^0}^2) + c_e^2 \tilde{B}_0(m_{\tilde{e}_2}^2, m_{\chi_i^0}^2)]. \end{aligned} \quad (3.33)$$

The two loop functions entering these expressions, I and \tilde{B}_0 , are given by

$$\begin{aligned} I(x, y, z) &= \frac{xy \ln x/y + yz \ln y/z + xz \ln z/x}{(x-y)(y-z)(x-z)}, \\ \tilde{B}_0(x, y) &= \frac{x \ln x - y \ln y}{x-y}, \end{aligned} \quad (3.34)$$

where the tilde in \tilde{B}_0 serves to distinguish this ‘‘truncated’’ version⁴ of the Passarino–Veltman function [39] (following the definitions of [40]).

Let us briefly discuss these results. Firstly, to gain some intuition on the relative contributions, it is instructive to consider a limiting case, where the left–right mixing is considered a perturbation. The dominant corrections arise from $(\Delta m_{(d,s,b)})_{\lambda_3}$ and $(\Delta m_b)_{\chi^+}$. For the first of these, taking $m_3 \sim m_{\tilde{d}_1} \sim m_{\tilde{d}_2}$, we have (for $d = (d, s, b)$)

$$\left(\frac{\Delta m_d}{m_d} \right)_{\lambda_3} \sim \frac{\alpha_s}{3\pi} \frac{m_3}{m_{\tilde{d}}^2} (\mu \tan \beta + A^*). \quad (3.35)$$

The contribution of these threshold corrections to δ_d arises only from $\text{Im}(\mu)$, as the contribution from $\text{Im}(A)$ is cancelled in constructing $\delta_d^{(m)} - \delta_d^{(H)}$. From (3.35), we see that when μ is negative ($\theta_\mu = \pi$) there is destructive interference with the tree-level mass term.

The presence of an extra diagram sets the b flavor apart from d and s , for which the following relation is expected if the soft-breaking sector is flavor-blind:

$$\frac{\Delta m_d}{m_d} = \frac{\Delta m_s}{m_s}, \quad \text{and} \quad \delta_d = \delta_s. \quad (3.36)$$

For the b quark mass, in a regime where the gaugino–higgsino mixing is also small, namely $\mu, m_i \gg m_w$ with m_i being the gaugino masses, we also find

$$\left(\frac{\Delta m_b}{m_b} \right)_{\chi^+} \sim -\frac{(Y_t^{SM})^2}{32\pi^2} \frac{\mu^* A_t^*}{m_t^2} \tan \beta, \quad (3.37)$$

⁴Note that the expression for \tilde{B}_0 requires a regulator scale. However, our physical results do not depend on this scale.

which indicates that when μ is real and positive, so that $(\Delta m_{(d,s,b)})_{\lambda_3}$ is real, the contribution to δ_b is positive when $0 < \theta_A < \pi$.

As is apparent from the limiting cases above, we observe the appearance of the reparametrization invariant CP-violating phases. In particular, at large $\tan \beta$

$$\phi_d \longrightarrow \theta_\mu + \pi, \quad (3.38)$$

where $\theta_\mu \equiv \text{Arg}(\mu)$, such that the CP-odd phase entering the gluino expression is $\text{Arg}(\mu m_3)$. The analogous behavior of the neutralino contributions is seen most easily in the limit $\mu, m_i \gg m_w$. Then,

$$N_{i1}^* \longrightarrow \delta_{i1} e^{-\frac{i}{2}\text{Arg} m_1}, \quad (3.39)$$

and the consequent CP-odd phase in the gaugino piece of the neutralino contribution is $\text{Arg}(\mu m_1)$ (or $\text{Arg}(\mu \sqrt{m_1 m_2})$). For the higgsino contribution, the relevant phase is $\text{Arg}(A\mu) \equiv \theta_A + \theta_\mu$.

It is worth noting that the origin of the $\tan \beta$ -enhancement, which is not manifest in the general expressions. For the gaugino contributions proportional to the I -function, this arises implicitly via the relation

$$m_{\tilde{d}_1}^2 - m_{\tilde{d}_2}^2 \propto m_d \tan \beta \quad (3.40)$$

at large $\tan \beta$, whereas the mixing angle stays constant in this limit.

The $\tan \beta$ enhancement of the amplitudes involving the \tilde{B}_0 function deserves special discussion. The relevant diagrams in the mass eigenstate basis appear to be divergent since they are proportional to the Passarino–Veltman B_0 function. However their $\tan \beta$ -enhanced imaginary parts are finite. As an example, let us consider the chargino contribution which involves gaugino–higgsino mixing. The relevant expression appearing in the amplitude is

$$\mathcal{G} = \frac{1}{\cos \beta} \sum_i U_{i2}^* V_{i1}^* m_{\chi_i^+} \tilde{B}_0(m_{\tilde{u}_1}^2, m_{\chi_i^+}^2). \quad (3.41)$$

There are in fact several compensating factors of $\tan \beta$ in this expression. To see this, we note that Eq.(3.27) implies

$$U^* f \left[M_{\chi^+} M_{\chi^+}^\dagger \right] M_{\chi^+} V^\dagger = f \left[\text{diag}(m_{\chi_1^+}^2, m_{\chi_2^+}^2) \right] \text{diag}(m_{\chi_1^+}, m_{\chi_2^+}) \quad (3.42)$$

for any (analytic) function f . Therefore,

$$\mathcal{G} = \frac{1}{\cos \beta} \left[\tilde{B}_0 \left(m_{\tilde{u}_1}^2, M_{\chi^+} M_{\chi^+}^\dagger \right) M_{\chi^+} \right]_{21}^* . \quad (3.43)$$

If \tilde{B}_0 here is replaced by a constant independent of M_{χ^+} , no $\tan \beta$ enhancement appears since $[M_{\chi^+}]_{21} = \sqrt{2} m_w \cos \beta$. This is the reason why the $\tan \beta$ -enhanced contribution is finite and the original Passarino–Veltman function gets replaced by its “truncated” version.

It is instructive to expand \tilde{B}_0 in powers of $(M_{\chi^+} M_{\chi^+}^\dagger - m_{\tilde{u}_1}^2)/m_{\tilde{u}_1}^2$ and extract the first $\tan\beta$ -enhanced term. Using the explicit form of the chargino mass matrix, one finds

$$\mathcal{G} \longrightarrow \frac{\mu^* m_2^*}{\sqrt{2} m_{\tilde{u}_1}^2} m_w \tan\beta. \quad (3.44)$$

This result can be understood via the mass-insertion approximation [41, 42]. To obtain $\tan\beta$ enhancement, it is necessary to introduce three mass insertions on the chargino line: μ – to mix \tilde{H}_1 with \tilde{H}_2 , $m_w \sin\beta$ – to mix the higgsinos and gauginos, and m_2 – to get the chirality flip in the diagram. Similar considerations apply to the neutralino contributions. We note that analogous calculations have been performed in Refs.[42] and [43].

(iii) Scalar-pseudoscalar mixing

The computation of $H - A$ mixing is straightforward, especially in the limit $m_A^2 \gg \langle AH \rangle$ [44]. Non-negligible contributions arise only from stop, sbottom and stau loops:

$$\begin{aligned} \langle AH \rangle = & \frac{3}{8\pi^2 v^2} \left[\frac{m_t^4 |\mu|^2 |A_t|^2}{(m_{\tilde{t}_1}^2 - m_{\tilde{t}_2}^2)^2} E(m_{\tilde{t}_2}^2/m_{\tilde{t}_1}^2) \sin(2\theta_{A_t} + 2\theta_\mu) \right. \\ & + \frac{m_b^4 |\mu|^2 |A_b|^2 \tan^4 \beta}{(m_{\tilde{b}_1}^2 - m_{\tilde{b}_2}^2)^2} E(m_{\tilde{b}_2}^2/m_{\tilde{b}_1}^2) \sin(2\theta_{A_\tau} + 2\theta_\mu) \\ & \left. + \frac{m_\tau^4 |\mu|^2 |A_\tau|^2 \tan^4 \beta}{3(m_{\tilde{\tau}_1}^2 - m_{\tilde{\tau}_2}^2)^2} E(m_{\tilde{\tau}_2}^2/m_{\tilde{\tau}_1}^2) \sin(2\theta_{A_\tau} + 2\theta_\mu) \right], \end{aligned} \quad (3.45)$$

where the loop function is given by $E(a) = -2 + (a+1)(a-1)^{-1} \ln a$. At moderate $\tan\beta$ the stau and sbottom contributions are heavily suppressed due to the factor of $m_{b(\tau)}^4$ in the numerator. However, this is not true at large $\tan\beta$, as the fourth power of $\tan\beta$ can overcome this suppression.

It is important to note that $\langle AH \rangle$ is even under flipping the sign of A , unlike the effects of the vertex corrections. Thus, these two sources can interfere *constructively* or *destructively*, depending on the position in parameter space. For example, choosing $\theta_\mu = 0$ and $0 < \theta_A < \pi/2$ leads to destructive interference between $C_{ij}^{(vc)}$ and $C_{ij}^{(AH)}$.

4 Synopsis of the EDM formulae

In this section, we compile the different contributions into physical observables measured in various EDM experiments. Such observables can be subdivided into three main categories: EDMs of paramagnetic atoms and molecules, EDMs of diamagnetic atoms, and the neutron EDM.

4.1 EDMs of paramagnetic atoms – thallium EDM

Among various paramagnetic systems, the EDM of the thallium atom currently provides the best constraints on fundamental CP violation and is often interpreted directly in terms

of the EDM of the electron. We therefore specialize our analysis to the case of Tl, noting that the conditions making C_{ij} important for thallium will also be applicable to other paramagnetic systems such as the YbF and PbO molecules, where significant experimental improvements in EDM measurements are likely [7, 8].

The semileptonic four-fermion operators (2.4) induce the following T-odd nucleon-electron interactions⁵ [9],

$$\mathcal{L}_{eN} = C_S \bar{e} i \gamma_5 e \bar{N} N + C_P \bar{e} e \bar{N} i \gamma_5 N + C_T \epsilon_{\mu\nu\alpha\beta} \bar{e} \sigma^{\mu\nu} e \bar{N} \sigma^{\alpha\beta} N, \quad (4.46)$$

where the isospin dependence is suppressed. Among these couplings, C_S plays by far the most important role for the EDM of paramagnetic atoms because it couples to the spin of the electron and is enhanced by the large number of nucleons in heavy atoms.

A number of atomic calculations [45, 46, 47] (see also Ref. [9] for a more complete list) have established the relation between the EDM of thallium, d_e , and the coefficients of the CP-odd electron-nucleon interactions C_S :

$$d_{\text{Tl}} = -585 d_e - e \text{ 43 GeV} \times (C_S^{\text{sing}} - 0.2 C_S^{\text{trip}}). \quad (4.47)$$

The relevant atomic matrix elements are calculated to within 10–20% accuracy [48]. Here the relative contribution of the isospin-triplet coupling is suppressed by $(N - Z)/A \simeq 0.2$, and the effects of C_P and C_T are negligible.

Before turning to the contributions to C_S , we recall for completeness (and to fix our conventions) that the electron EDM d_e receives a number of well-known contributions from superpartner loops. At one-loop order, threshold corrections from $\tilde{e} - \chi^+$ and $\tilde{e} - \chi^0$ loops dominate, and we follow the notation of Ibrahim and Nath [14] for these terms (up to a different convention for the squark mixing angles as specified earlier). At two-loop order, non-negligible Barr-Zee-type Higgs-mediated graphs contribute [49], where CP violation enters through the couplings of (s)fermions to the pseudoscalar Higgs A . We follow the work of Chang, Keung and Pilaftsis [49] (though our phase conventions are somewhat different) and to emphasize an additional contribution, we quote the full expression below:

$$d_e^{\text{two-loop}} = |e| Q_e \frac{\alpha_{em}}{32\pi^3} \frac{m_e}{m_A^2} \sum_{j=t,b,\tau} \zeta_j Q_j^2 N_j \left[F\left(\frac{m_{\tilde{j}_1}^2}{m_A^2}\right) - F\left(\frac{m_{\tilde{j}_2}^2}{m_A^2}\right) \right] \tan \beta, \quad (4.48)$$

where $j = t, b, \tau$ are flavors running in the sfermion loop. $N_t = N_b = 3$, and $N_\tau = 1$, accounts for the trace over color, while the two-loop function $F(z)$ is given explicitly in [49]. The CP-violating couplings in our conventions are:

$$\zeta_j = \frac{\sin(2\theta_j) m_j R_j \text{Im}(\mu e^{-i\phi_j})}{v^2 \sin \beta \cos \beta}, \quad (4.49)$$

Note that while there are in principle a large number of possible diagrams in this class [50], those containing stop, sbottom, and stau loops should be dominant at large $\tan \beta$. We

⁵Note that we differ from Ref. [9] in the definition of γ_5 , so that we use $P_L = (1 - \gamma_5)/2$.

emphasize here that the stau-loop contribution, which has hitherto been neglected in the literature, is a significant addition – in fact for the CMSSM and NUHM at $\tan\beta = 50$ to be considered here, it often provides the dominant contribution due to the generically light staus.

In order to see the dependence on the reparametrization invariant phases, it is useful to again consider the small-mixing regime where $m_L^2 \sim m_R^2 \gg m_A^2, m_{LR}^2$. For large $\tan\beta$, the EDM then reduces to

$$d_e^{\text{two-loop}}(j = t, b, \tau) \sim -Q_j^2 N_j (Y_j^{SM})^2 \frac{\alpha_{em} m_e |\mu A_j|}{192\pi^3 m_j^4} \ln \left(\frac{m_j^2}{m_A^2} \right) \sin(\theta_{A_j} + \theta_\mu) \tan^n \beta, \quad (4.50)$$

where we used $Q_e = -1$, and defined n as $n = 1$ for $j = t$ and $n = 3$ for $j = b, \tau$. It is important to recognize that when $\theta_\mu = 0$ the two-loop contribution to the electron EDM is negative which interferes destructively with the one-loop contribution referred to above⁶.

Having accounted for d_e , the calculation of C_S induced by (2.4) follows from the low-energy theorem that expresses the nucleon matrix element of $\alpha_s G_{\mu\nu} G^{\mu\nu}$ in terms of the mass of the nucleon and the QCD beta function [52]. As a consequence of this theorem, for a heavy quark Q , $\langle N | m_Q \bar{Q} Q | N \rangle \simeq 70$ MeV. This theorem is valid in the exact chiral limit, and thus receives corrections from the non-zero values of the light quark masses. Following [26], we parametrize the $m_s \bar{s}s$ matrix element as $\kappa \equiv \langle N | m_s \bar{s}s | N \rangle / 220$ MeV. Using this parametrization, as well as the measured value of $(m_u + m_d) \langle N | \bar{u}u + \bar{d}d | N \rangle / 2 \simeq 45$ MeV and the ratio of the quark masses $m_u/m_d \simeq 0.55$, we arrive at the following general formula for C_S in terms of C_{qe} ,

$$\begin{aligned} C_S^{sing} &= C_{de} \frac{29 \text{ MeV}}{m_d} + C_{se} \frac{\kappa \times 220 \text{ MeV}}{m_s} + C_{be} \frac{66 \text{ MeV}(1 - 0.25\kappa)}{m_b}, \\ C_S^{trip} &\sim -C_{de} \frac{1 - 3 \text{ MeV}}{m_d}. \end{aligned} \quad (4.51)$$

In this formula, C_{de}/m_d and C_{se}/m_s should be taken at the normalization scale 1 GeV, while C_{be}/m_b must be normalized at m_b . In the case of minimal SUSY models, these combinations are scale invariant, as $C_{qe} \sim m_q$. There is a rather large uncertainty in the isospin triplet coupling due to the poorly known value of $(m_d - m_u) \langle p | \bar{u}u - \bar{d}d | p \rangle$. Fortunately, C_S^{trip} is numerically small and a further suppression via (4.47) makes the contribution of C_S^{trip} completely negligible for all applications. Thus, from now on, we neglect C_S^{trip} and drop the superscript in C_S^{sing} .

The largest uncertainty in C_S (4.51) that may significantly affect numerical values of EDMs originates from the poorly known value of κ . The assumption that the s quark behaves as a heavy quark would give $\kappa \simeq 0.3$, which we regard as a lower bound. The analysis of the baryon octet mass splitting at leading order in chiral perturbation theory instead suggests $\kappa \simeq 1$, while an improved next-to-leading order calculation gives a prediction $\kappa \simeq 0.50 \pm 0.25$ [53] that we use as the central point for our numerical analysis. From

⁶Note that Barr-Zee-type diagrams with chargino loops also contribute for $\theta_\mu \neq 0$ [51, 37].

these numbers it is clear that the overall precision with which this matrix element can be estimated is not better than 30%.

Substituting Eqs. (3.22) and (3.24) into (4.51), we arrive at the final expression for C_S in terms of m_A , Δm_i , δ_i and $\langle AH \rangle$:

$$C_S \simeq -\frac{5.5 \times 10^{-10} \tan^2 \beta}{m_A^2 |1 + \Delta m_e/m_e^{(0)}|} \left[\frac{(1 - 0.25\kappa)}{|1 + \Delta m_b/m_b^{(0)}|} \left(\sin(\delta_b - \delta_e) - \frac{\langle AH \rangle}{m_A^2} \right) \right. \\ \left. + \frac{3.3\kappa}{|1 + \Delta m_s/m_s^{(0)}|} \left(\sin(\delta_s - \delta_e) - \frac{\langle AH \rangle}{m_A^2} \right) \right. \\ \left. + \frac{0.5}{|1 + \Delta m_d/m_d^{(0)}|} \left(\sin(\delta_d - \delta_e) - \frac{\langle AH \rangle}{m_A^2} \right) \right]. \quad (4.52)$$

We use this calculation of C_S , along with the standard SUSY calculations of d_e reviewed above, in the analysis of the thallium EDM as a function of SUSY masses and phases which will be discussed in Section 5.

4.2 Neutron EDM

The calculation of the neutron EDM in terms of the Wilson coefficients of Eq. (2.5) represents a difficult non-perturbative problem. The most common approach invokes “naive dimensional analysis” (NDA) [54, 55] which gives an order of magnitude estimate for $d_n(d_i, \tilde{d}_i, w)$ with uncertain signs. Some partial calculations have also been performed with the use of chiral perturbation theory [56, 57] and lattice QCD [58]. Recently, a universal treatment of all operators within the same method was developed in Refs. [59, 60] using QCD sum rule techniques. We briefly summarize these results below.

It is natural to expect that the dominant contribution to the neutron EDM comes from the EDMs and color EDMs of u and d quarks. We recall that the $\bar{\theta}$ -dependence is removed by the Peccei-Quinn mechanism, which at the same time reduces the contribution of the color EDM of the s -quark [59]. The QCD sum rule analysis [59] leads to the following result:

$$d_n(d_i, \tilde{d}_i) = 0.7(d_d - 0.25d_u) + 0.55e(\tilde{d}_d + 0.5\tilde{d}_u), \quad (4.53)$$

where the value of the quark vacuum condensate $\langle \bar{q}q \rangle = (225 \text{ MeV})^3$ has been used. Here \tilde{d}_q and d_q are to be normalized at the hadronic scale which we assume to be 1 GeV. The relation to the Wilson coefficients at the weak scale is as follows,

$$\tilde{d}_q(1 \text{ GeV}) \simeq 0.91\tilde{d}_q(M_Z); \quad d_q(1 \text{ GeV}) \simeq 1.2d_q(M_Z). \quad (4.54)$$

Note that \tilde{d}_q as defined by Eq. (2.2) has a much milder QCD scaling than an alternative definition for \tilde{d}_q which includes a factor of g_s in its definition. The reader should also note that the quark masses used for the SUSY calculations of d_q and \tilde{d}_q should be taken at the weak scale, where their numerical values are smaller than the low energy values by a factor of ~ 0.35 , *e.g.* $m_d(M_Z) \simeq 9.5 \text{ MeV} \times 0.35$.

The expression (4.53) has several nice features. Its flavor composition agrees with the predictions of the SU(6) constituent quark model, while the proportionality to $d_q \langle \bar{q}q \rangle \sim m_q \langle \bar{q}q \rangle \sim f_\pi^2 m_\pi^2$ removes any sensitivity to the absolute value of the light quark mass. The quark EDM part of (4.53) is in good agreement with lattice calculations [58]. Finally, the overall uncertainty of (4.53) is estimated to be at the 30%–50% level [59]. For completeness, we recall that there are standard SUSY one- and two-loop contributions to d_q and \tilde{d}_q in analogy with those discussed for the electron EDM above. For 1-loop quark EDMs and CEDMs we follow [14] and note that, in comparison to the electron EDM, for quarks there are additional one-loop diagrams containing squark-gluino loops. The two-loop Barr-Zee–type contributions to the quark EDMs [49] also receive a significant correction from the stau-loop in addition to those containing stops and sbottoms.

The Weinberg operator can also be an important source of CP violation, especially when the third generation of squarks is lighter than the first two generations. Unfortunately, a reliable calculation of its contribution to the neutron EDM is problematic at this point. The QCD sum rule approach [60] produces an estimate that is close to the NDA result but this calculation is at the border-line of applicability of the method. With w normalized at the 1 GeV scale one finds:

$$d_n(w) \sim 20 \text{ MeV} \times e w. \quad (4.55)$$

This estimate is assessed to be valid within a factor of 2–3 [60]. However, it seems unlikely that this uncertainty can be significantly reduced. An important implication is then that even the sign cannot be reliably inferred, as the next order corrections to the QCD sum rule determination (4.55) are not calculable and plausibly are large.

When $\tan \beta$ is large, we expect that a generically dominant contribution to the Weinberg operator will be induced by the b -quark color EDM (see also [61, 62]). Thus, the expression for $w(\tilde{d}_b)$ linearly enhanced by $\tan \beta$ takes the form:

$$w(1 \text{ GeV}) = 0.72 w(m_b) = -0.72 \times \frac{g_s^3 \tilde{d}_b(m_b)}{32\pi^2 m_b} = -0.68 \times \frac{g_s^3 \tilde{d}_b(M_Z)}{32\pi^2 m_b}. \quad (4.56)$$

It is well known that the t and c quark two-loop contributions are just a fraction of the total EDM at low $\tan \beta$ [63]. Since they do not grow with $\tan \beta$, their effect is expected to be negligible but nonetheless they are included in our analysis. We remark at this point that it is common in the SUSY-EDM literature to quote the Weinberg operator at the hadronic scale as $3.3 \times w(M_Z)$. This relation originates from Ref. [62] where the contributions to w induced by \tilde{d}_b and \tilde{d}_c were added at the b and c thresholds with some specific assumptions about the SUSY spectrum and a fixed (rather low) value of $\tan \beta$. For any other point in the parameter space this coefficient is going to be different, and therefore an explicit summation of the b and c thresholds should be performed separately.

There are many different types of four-fermion operators generated via the vertex correction mechanism that contribute to the neutron EDM at leading order: C_{ds} , C_{sd} , C_{bd} , C_{db} , C_{bs} , and C_{sb} . The contribution of the first two operators to d_n could be important a priori [35]. We note, however, that the CP-violating phases induced under renormalization are the same for the d and s quarks to very high accuracy within the framework of a flavor-blind

soft-breaking sector. Thus, $\delta_s \approx \delta_d$ and $C_{ds} \approx -C_{sd} \approx 0$, from Eq. (3.36). This however does not apply to C_{bd} and C_{db} or C_{bs} and C_{sb} due to an additional chargino contribution to the b -quark mass. The estimates of d_n induced by C_{bd} and C_{db} can be obtained along the lines of Ref. [60]. We supply some of the details of this calculation in Appendix B, and quote here the result:

$$d_n(C_{bd}) \sim \frac{e \cdot 0.65 \times 10^{-3} \text{GeV}^2}{m_b} C_{bd}, \quad (4.57)$$

where we took into account that $C_{bd} \simeq -C_{db}$. The Yukawa couplings Y_d and Y_b that enter the coefficient C_{bd} in (4.57) are normalized at 1 GeV and m_b respectively. In the final result for d_n , C_{bs} and C_{sb} may be as important as C_{bd} and C_{db} . However, we are not aware of any reliable way to estimate $d_n(C_{bs}, C_{sb})$.

Combining the different contributions, (4.53), (4.55) and (4.57), we arrive at a final formula for the neutron EDM as a function of the different Wilson coefficients:

$$d_n = d_n(d_q, \tilde{d}_q) + d_n(w) + d_n(C_{bd}). \quad (4.58)$$

One should keep in mind at this point that, as emphasized above, Eqs. (4.55) and (4.57) are undoubtedly of poorer precision than (4.53). Therefore, a reliable calculation of d_n in terms of a specific combination of SUSY CP-violating phases is possible only if both the second and third terms in (4.58) are smaller than $d_n(d_q, \tilde{d}_q)$. When instead they contribute at a level comparable to the EDMs and color EDMs of quarks, an interpretation of the neutron EDM bound in terms of constraints on specific CP-violating phases becomes problematic.

4.3 EDMs of diamagnetic atoms – mercury EDM

EDMs of diamagnetic atoms, i.e. atoms with total electron angular momentum equal to zero, also provide an important test of CP violation [9]. The current limit on the EDM of mercury [3] furnishes one of the most sensitive constraints on SUSY CP-violating phases [16]. However, the calculation of d_{Hg} is undoubtedly the most difficult as it requires QCD, nuclear, and also atomic input.

The atomic EDM of mercury arises from several important sources, namely, the Schiff moment S [64], the electron EDM d_e , and also the electron-nucleus interactions C_S and C_P (see, e.g. Ref. [9] for a comprehensive review). Schematically, the mercury EDM can be represented as

$$d_{\text{Hg}} = d_{\text{Hg}} \left(S[\bar{g}_{\pi NN}(\tilde{d}_i, C_{q_1 q_2})], C_S[C_{qe}], C_P[C_{eq}], d_e \right), \quad (4.59)$$

where $\bar{g}_{\pi NN}$ collectively denotes the CP-odd pion-nucleon couplings. The atomic and nuclear parts of the calculation have been performed by different groups, and several results such as $d_{\text{Hg}}(S)$ [65] and $S(\bar{g}_{\pi NN})$ [66] have been updated recently. The most important numerical change comes from a new QCD sum-rule calculation of $\bar{g}_{\pi NN}(\tilde{d}_i)$ [67], that obtained a preferred range and “best” value for this coupling. Previous estimates [33, 16] are within this preferred range, but close to the largest possible value for the $\bar{g}_{\pi NN}(\tilde{d}_i)$ matrix element. The best value that follows from the sum-rule analysis [67] is a factor of $\sim 2.5 - 3$

smaller than previously used values [16]. Incorporating the changes in the atomic matrix elements, the current theoretical estimate for the mercury EDM induced by dimension 5 operators stands as:

$$d_{\text{Hg}} = 7 \times 10^{-3} e(\tilde{d}_u - \tilde{d}_d) + 10^{-2} \times d_e. \quad (4.60)$$

Note that the electron EDM also contributes to d_{Hg} , although less significantly than to d_{Th} which provides a more stringent bound. Therefore, the most valuable feature of d_{Hg} is its sensitivity to the triplet combination of color EDM operators \tilde{d}_i , which surpasses the neutron EDM sensitivity to this combination of these operators by a factor of a few. The overall uncertainty in the QCD part of the calculation is considerably larger than that for the neutron due to significant cancellations, reflecting the fact that the result vanishes in the vacuum factorization approximation (see Appendix B). However, the dominant dependence on the $(\tilde{d}_u - \tilde{d}_d)$ combination ensures that these uncertainties enter as an overall factor and therefore do not significantly alter the shape of the unconstrained band of the parameter space in the $\theta_\mu - \theta_A$ plane.

One should note that the mercury EDM also receives contributions from the color EDM of the strange quark [16] and the EDMs of light quarks, although their contribution is subleading. Finally, the Weinberg operator does not provide any appreciable contribution to d_{Hg} because its contribution to $\bar{g}_{\pi NN}$ is suppressed by an additional chiral factor of $m_q/1 \text{ GeV} \sim 10^{-2}$.

At large $\tan \beta$ one should also include additional contributions to the Schiff moment coming from the four-quark operators, as well as the effects of the semi-leptonic operators C_S and C_P :

$$\begin{aligned} d_{\text{Hg}} = & 7 \times 10^{-3} e(\tilde{d}_u - \tilde{d}_d) + 10^{-2} d_e \\ & - 1.4 \times 10^{-5} e \text{ GeV}^2 \left(\frac{0.5 C_{dd}}{m_d} + 3.3 \kappa \frac{C_{sd}}{m_s} + \frac{C_{bd}}{m_b} (1 - 0.25 \kappa) \right) \\ & + 3.5 \times 10^{-3} \text{ GeV} e C_S + 4 \times 10^{-4} \text{ GeV} e C_P. \end{aligned} \quad (4.61)$$

The second line in (4.61) is the contribution of the four-quark operators to the Schiff moment. The details of the $\bar{g}_{\pi NN}(C_{q_1 q_2})$ estimates, based on a factorization assumption, are given in Appendix B. The result depends on the same parameter κ (the nucleon strangeness in the 0^+ channel) as the coefficient C_S . As emphasized before, C_{sd} and C_{dd} are not induced via vertex corrections, and arise only through $A - H$ mixing. Finally, the contribution of C_P is given primarily by C_{ed} [26] while the contributions from C_{es} and C_{eb} are consistent with zero. The QCD normalization of all operators is the same as in the thallium and neutron cases.

In the region of parameter space where the color EDM contribution to d_{Hg} is dominant, the mercury EDM limit is extremely valuable since, as noted above, it constrains the triplet combination of up and down color EDMs, and therefore a calculable combination of the CP-violating phases. On the other hand, when other terms in Eq. (4.61) contribute at a level comparable to that of $\tilde{d}_u - \tilde{d}_d$, which in fact is expected at large $\tan \beta$, different uncertainties no longer factorize in front of a given phase combination, and the interpretation of the mercury EDM constraint becomes more difficult.

5 Numerical analysis of EDMs at large $\tan \beta$

In this section we analyze all three observables, d_{Ti} , d_n and d_{Hg} , within two classes of MSSM models. In both cases we assume flavor-blind SUSY breaking, a common trilinear soft-breaking parameter A_0 , and a universal (real) gaugino mass parameter $m_{1/2}$ at the GUT scale. This narrows down the number of SUSY CP-violating phases to two, which can be identified with the phases of the μ and A_0 parameters. We then perform an EDM analysis separately for these two phases. In all numerical runs the value of $\tan \beta$ was chosen to be nearly maximal, $\tan \beta = 50$. We defer an analysis of the constraints on the SUSY CP-violating phases to a subsequent publication [68] and now focus on the relative importance of various EDM contributions.

The constrained MSSM (CMSSM) is a popular framework defined by the following set of universal SUSY parameters at the GUT scale:

$$\{\tan \beta, m_0, m_{1/2}, |A_0|, \theta_A, \theta_\mu\}. \quad (5.62)$$

The magnitude of the μ -parameter and the pseudoscalar mass are determined by the radiative electroweak symmetry breaking conditions (i.e. by reproducing the observed value of M_Z). We note that, in models with CP violation, the usual sign ambiguity of μ becomes a phase ambiguity.

The renormalization group running from the GUT scale introduces considerable mass splittings in the spectrum of superpartners. For example, the gluino becomes much heavier than (roughly triple) the rest of the gauginos. The RG running can also make the scalar quarks quite heavy,

$$m_{\text{sq}}^2(M_Z) \simeq m_0^2 + 6m_{1/2}^2 + O(M_Z^2), \quad (5.63)$$

especially if $m_{1/2}$ is large. In our analysis, the masses of the A and H Higgs bosons are functions of the above input parameters and are of particular importance. In the CMSSM with large $\tan \beta$, they tend to be as heavy as the sleptons. As a consequence, the parameter ξ determining the relative importance of the four-fermion operators (2.6) cannot be varied over a large range once $\tan \beta$ is fixed.

In contrast, ξ becomes a free parameter in another version of the MSSM, a CMSSM-type model with non-universal Higgs masses (NUHM). In this model the squarks and sleptons are still mass degenerate at the GUT scale, but the Higgs soft masses are not. The model differs from the CMSSM in having two additional Higgs mass parameters, which can be taken to be the mass of the pseudoscalar m_A and μ evaluated at the weak scale, so that the parameter set becomes

$$\{\tan \beta, m_0, m_{1/2}, m_A, |\mu|, |A_0|, \theta_A, \theta_\mu\}. \quad (5.64)$$

Relaxing the scalar mass universality brings an interesting new degree of freedom into weak-scale phenomenology while preserving the flavor-degeneracy of the CMSSM. For this study it is important that m_{slepton}/m_A and m_{squark}/m_A can be varied over a large range,

thus presenting an opportunity to study the transition to a regime of dominance for the four-fermion operators.

In what follows, we present our numerical results for the EDMs using three two-dimensional slices through the parameter space – planes of $m_{1/2}$ – m_0 (typical of the CMSSM) and μ – m_A and m_A – m_0 (as examples of the NUHM). For each EDM observable, we plot one CMSSM figure with $\theta_\mu = 0$ and $\theta_A = \pi/2$. Note that the phase of A runs in the RGEs, so that at low energies, the phases of the various A_i are different and those of the squarks are typically $\ll \pi/2$, whereas the phases of $A_{\tilde{l}}$ remain relatively large. In contrast, the phase of μ does not run so that $\theta_\mu(EW) = \theta_\mu(GUT)$. We also plot for each EDM, three different NUHM cases: one for $\theta_\mu = 10^{-3}\pi$ and $\theta_A = 0$ and two different parameter planes for $\theta_\mu = 0$ and $\theta_A = \pi/2$. In all cases we fix $\tan\beta = 50$ and $|A_0| = 300$ GeV as well as $m_t = 175$ GeV for the pole mass, and $m_b = 4.25$ GeV for the running \overline{MS} mass evaluated at m_b itself. Note that our results for the EDMs are not particularly sensitive to the choice of $|A_0|$.

In all cases, we apply a set of phenomenological constraints that we describe briefly. We apply the constraints on new particles from direct LEP searches, namely $m_{\chi^\pm} > 104$ GeV [69] and Higgs mass limits [10] of $m_h > 114$ GeV. The light Higgs mass has been computed using FeynHiggs [70]. We also require the calculated branching ratio for $b \rightarrow s\gamma$ to be consistent with experimental measurements [71]. For each set of parameters, we calculate the relic density of neutralinos having set the CP-violating phases to 0. As such the domains we display for a given relic density are only indicative. However, we note that in the CMSSM (and more generally when sfermion masses are not too degenerate at the weak scale), the relic density of binos is not significantly affected by these phases [13]. For the relic density of neutralinos χ , we show regions of the parameter planes with $0.1 \leq \Omega_\chi h^2 \leq 0.3$. We use this more conservative range in addition to that suggested by the recent WMAP data [72] ($0.094 \leq \Omega_\chi h^2 \leq 0.129$) for clarity in the figures. The effect of the WMAP densities in the CMSSM was discussed in [73] and in the NUHM in [74]. We also require that the lightest supersymmetric particle (LSP) be a neutralino. For further details on these constraints see [75].

5.1 Thallium EDM

As emphasized in section 4.1, the thallium EDM receives two main contributions at large $\tan\beta$, from d_e and C_S , while the EDM of the electron itself can be generated in different ways at both one- and two-loop order. Figure 4a plots contours of constant $d_{\text{Ti}}(C_S)/d_{\text{Ti}}$ (solid, blue) and $d_e^{2\text{-loop}}/d_e^{\text{total}}$ (dashed, red) in the CMSSM as a function of $m_{1/2}$ and m_0 . The GUT-scale phase of A_0 is set to be maximal, $\theta_A = \pi/2$, while $\theta_\mu = 0$. The dark (red) shaded lower-right half of the plane corresponds to a stau-LSP region which is excluded if the LSP is stable. The medium (green) shaded region is excluded by $b \rightarrow s\gamma$ (computed with non-zero phases). In the broad light shaded region the relic density of neutralinos is $0.1 < \Omega h^2 < 0.3$ (computed in the absence of phases) and the thin slightly darker region shows the WMAP relic density. In this figure, the relic density is determined primarily by co-annihilations with the nearly degenerate $\tilde{\tau}$ and/or strong s-channel annihilation through

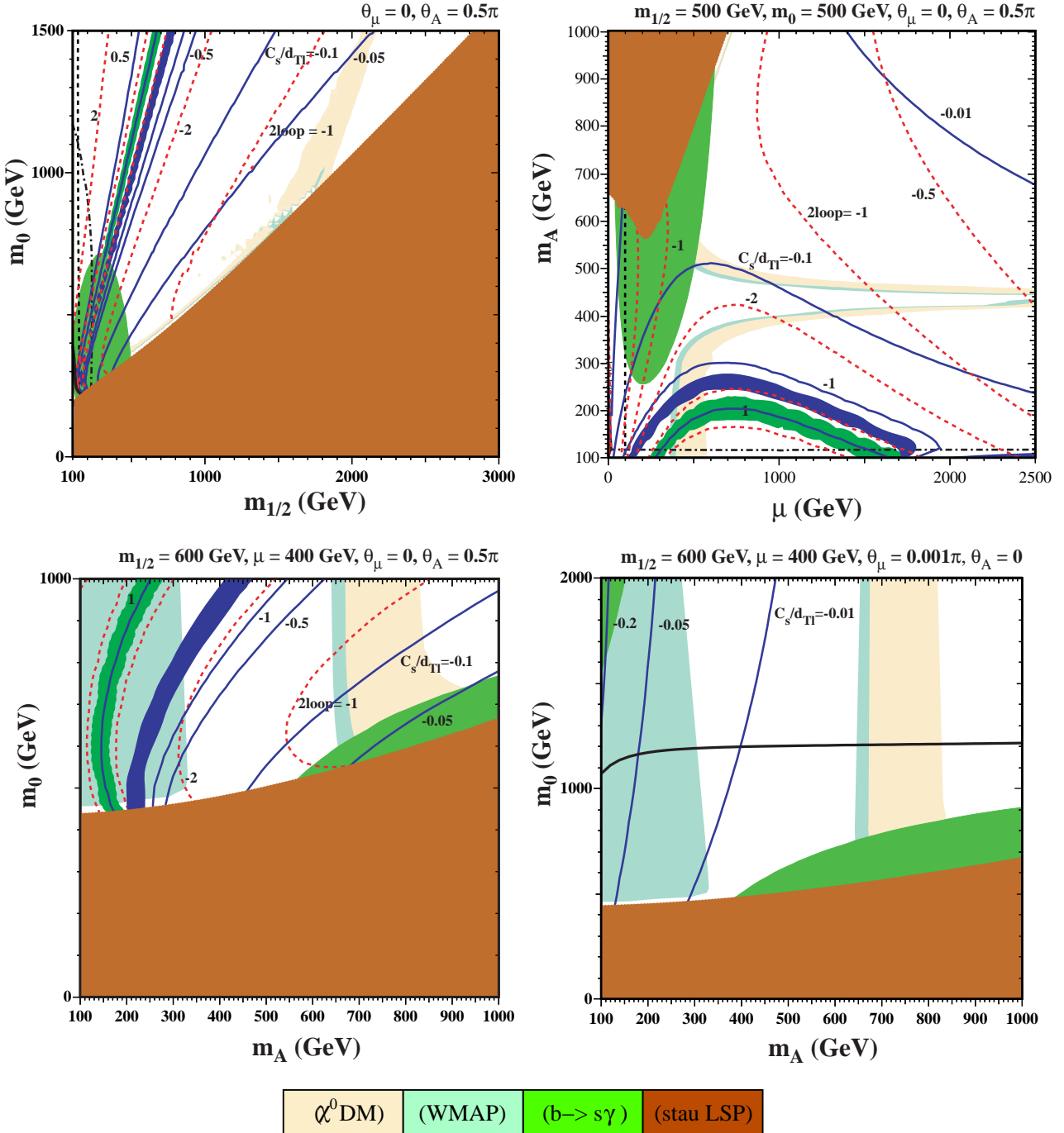


Figure 4: Contributions of four-fermion operators (C_S) and the electron EDM (d_e) to the EDM of thallium as functions of the SUSY parameters. Blue (solid) lines are contours of constant $d_{\text{Tl}}(C_S)/d_{\text{Tl}}$, and red (dashed) lines are the contours of constant $d_e^{2\text{-loop}}/d_e^{\text{total}}$. A thick solid black line marks the current experimental constraint on $|d_{\text{Tl}}|$, and black dashed and dot-dashed lines represent constraints from direct searches for charginos and the Higgs. The legend indicates the color(grey-scale)-coding of the excluded regions and preferred domains as described in the text.

the heavy Higgses H, A . In almost all of the unshaded portions of this figure, the relic density is too high and these parameter choices would be excluded if the LSP is stable. Also shown by the nearly vertical black dashed line is the LEP bound on the chargino mass (smaller values of $m_{1/2}$ are excluded) and the black dot-dashed curve is the LEP bound on the Higgs mass (which also excludes small values of $m_{1/2}$ and m_0).

The importance of C_S and d_e^{2-loop} grow as one moves to lower $m_{1/2}$ and higher m_0 as indicated by the blue (solid) and red (dashed) lines. In particular, the contribution from C_S changes dramatically, from merely a 5% effect to a 100% contribution, while the two-loop contributions are generically large. Moreover, since the effects of C_S and d_e^{2-loop} have the opposite sign relative to the one-loop contribution to d_e , the overall consequence is a significant *reduction* of the predicted observable thallium EDM over a large portion of the parameter space. In fact, the total EDM of thallium is generically several times smaller than either $d_{\text{Ti}}(C_S)$ or $d_{\text{Ti}}(d_e^{total})$ individually. The band in parameter space where there is greater than 80% cancellation between C_S and d_e is shaded in blue (dark grey), i.e., $d_{\text{Ti}}(C_S)/d_{\text{Ti}} > 5$. In the center of this band, d_{Ti} actually vanishes. Our results for C_S are weakly dependent on κ . The 50% uncertainty in κ , translates into a 10% uncertainty in C_S . This lack of sensitivity to κ can be inferred from Eq. (4.52) where the first term in the square bracket is dominant.

As noted earlier, the importance of the two-loop d_e contribution stems primarily from stau loops since the staus are generically lighter than the rest of the squarks and sleptons. The left-most band, shaded green (light grey), in the parameter space shows the region where these two-loop contributions nearly screen the one-loop effects in d_e (to 95%). In this band, $d_e^{2-loop}/d_e > 20$. In the center of the band, $d_e = 0$ and the observable atomic EDM is given entirely by C_S . Note that C_S is dominated by vertex corrections, $C_{ij}^{(vc)}$, and the contribution due to H - A mixing is not very important.

Turning now to the NUHM, we observe that the cosmologically preferred region of parameter space can be substantially wider. Figure 4b presents the thallium EDM results in the $\mu - m_A$ plane, and one can see that even for m_A as high as 500 GeV C_S may contribute 10% of the total thallium EDM, while for $m_A < 300$ GeV C_S often provides the dominant contribution. Here, we have fixed $m_{1/2} = m_0 = 500$ GeV. For this choice of parameters, positivity of the Higgs soft masses at the GUT scale would require $\mu \lesssim 1600$ GeV [30]. In this figure, the $\tilde{\tau}$ -LSP region is now in the upper left corner and the region excluded by $b \rightarrow s\gamma$ extends down from that. The region with the relic density between 0.1 and 0.3 are the two funnel-like strips which become nearly horizontal at large μ . This region is allowed by the rapid s-channel annihilation of χ 's through heavy H, A . Note that $m_\chi \approx 0.4m_{1/2} \approx m_A/2$ here. Between these two strips, the relic density is less than 0.1 and so is not excluded. The WMAP region corresponds to the thin strips in the interior of the funnel. Once again, we see the blue band with $d_{\text{Ti}}(C_S)/d_{\text{Ti}} > 5$ at $m_A \lesssim 250$ GeV which now intersects the WMAP region at $\mu \sim 400$ GeV and $m_A \sim 200$ GeV. At slightly lower m_A , the 2-loop contribution cancels the 1-loop contribution to d_e and $d_{\text{Ti}} = d_{\text{Ti}}(C_S)$.

Perhaps the most interesting slice to consider is the $m_A - m_0$ plane plotted in Fig. 4c. From Fig. 4b, we see that in order to maximize the size of the WMAP cosmological region,

we should choose $\mu = 400$ GeV. Here, $m_{1/2}$ is fixed to 600 GeV. Indeed, in Figs 4c and 4d, we see a large region with $m_A \lesssim 300$ GeV (and $m_A \sim 650$ GeV) where $\Omega_\chi h^2 \approx 0.11$. For intermediate values of m_A the relic density is small and a dark matter candidate is not provided. The $\tilde{\tau}$ -LSP region now excludes the lower portion of the figure and $b \rightarrow s\gamma$ excludes a small area at higher m_0 when m_A is large.

In Fig. 4c, one can see that over most of the cosmologically preferred region, C_S provides the dominant contribution to the atomic EDM. It follows that nowhere within this region can the observable EDM be interpreted purely in terms of d_e alone. Moreover, one observes that within the same cosmologically preferred region there is a large band of the parameter space where the two contributions to the total atomic EDM cancel, implying no constraint on the CP-violating phase. Once again, 50% changes in κ lead to 10% changes in C_S . The final figure (4d) presents the same slice of parameter space within the NUHM as Fig. 4c for $\theta_A = 0$ and $\theta_\mu = 10^{-3}\pi$. In this regime, the one-loop contribution to d_e is $\tan\beta$ -enhanced, and provides the dominant effect. We see that even for $\theta_\mu \sim \mathcal{O}(10^{-3})$ the domain of parameter space with $m_0 \lesssim 1100$ GeV is excluded by the thallium EDM bound as shown by the thick solid black curve. The contribution of C_S reaches 20% on this plot for low m_A and high values of m_0 . Clearly, in this case, over the range of parameter space that is potentially accessible at future colliders, the one-loop electron EDM provides the leading contribution to the atomic EDM of thallium. Here, we note that when $\theta_\mu \neq 0$, the sensitivity to κ is larger and a 50% change in κ leads to a comparable change in C_S .

In summary, this numerical analysis indicates that although C_S plays a very important role for paramagnetic EDMs at large $\tan\beta$, the precise values are somewhat (a factor of a few) smaller than one would naively expect from the simple scaling arguments presented in Sec. 2. The main reason for this is that C_S is driven mostly by squark loops while d_e also receives contributions from selectrons, and as a consequence C_S tends to be further suppressed due to the generically heavy masses of the squarks. Another important factor is the renormalization group evolution from the GUT scale down to the electroweak scale that considerably suppresses the size of $\text{Im}A_t$ relative to $\text{Im}A_e$ leading to an additional suppression of C_S/d_e .

5.2 Neutron EDM

Repeating the same sequence of plots for the neutron EDM, we observe important differences with respect to thallium. In all four panels of Fig. 5, the phenomenological and cosmological considerations are identical to those described for Fig. 4. In the CMSSM, with $\theta_A = \pi/2$, the current experimental bound, shown as the thick black curve, for d_n excludes much more of the plane than that for d_{TI} (due to the absence of any significant cancellations). Indeed, for low values of $m_{1/2}$ around 100 GeV, scales for m_0 above 1 TeV are probed by the experimental constraint. In the other planes, the choices for $m_{1/2}$ and m_0 and/or μ were made so as to satisfy ab initio the current experimental bounds over the displayed plane. Furthermore, there is little sensitivity to $\theta_\mu = 10^{-3}\pi$ compared to that of the thallium EDM. The contribution of the two-loop quark EDMs and CEDMs is in gen-

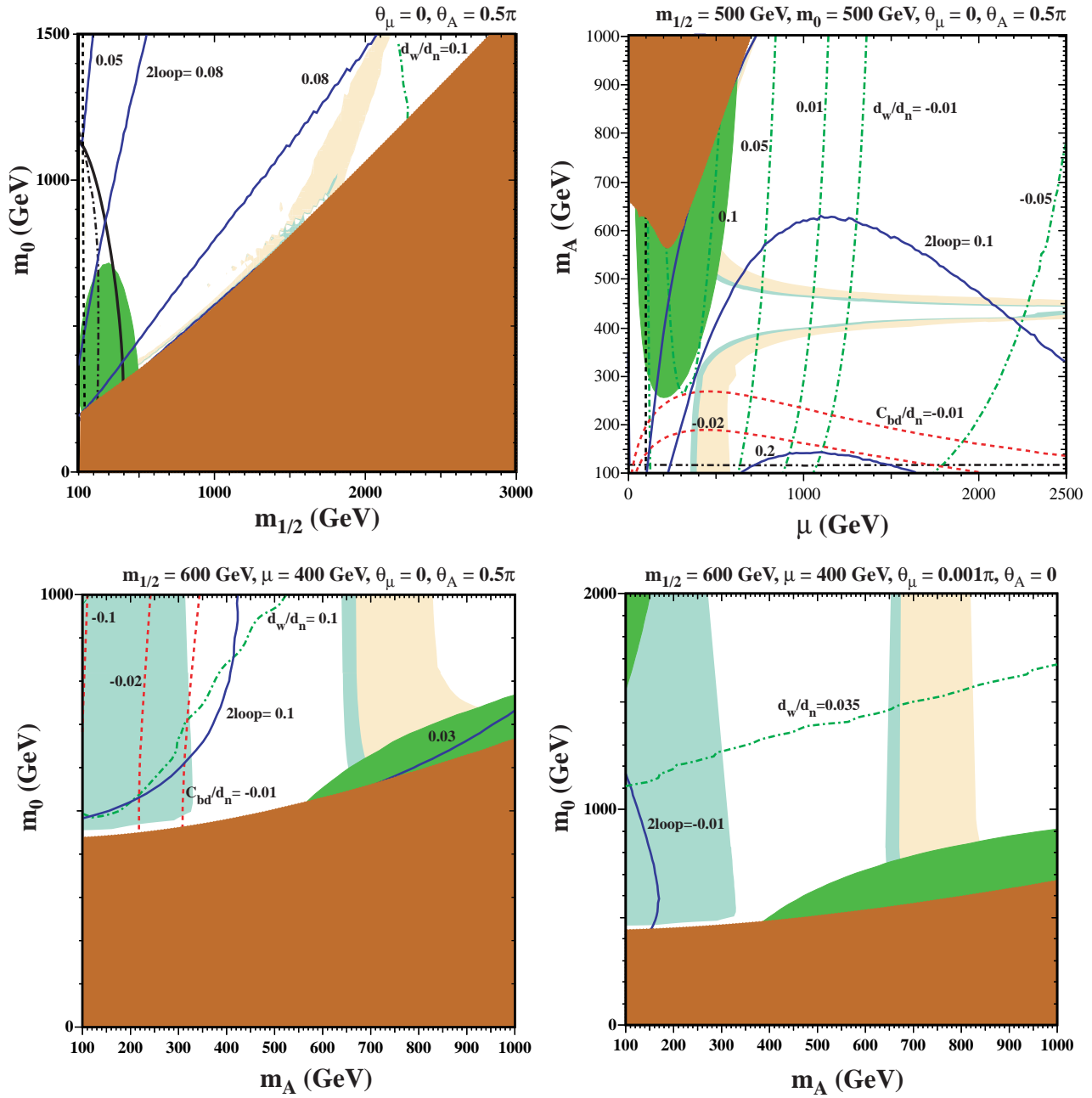


Figure 5: Contributions of the Weinberg operator, $d_n(w) \equiv d_w$, and four-fermion operators, $d_n(C_{ij})$ denoted as C_{bd} here, to the neutron EDM as functions of SUSY parameters. Blue (solid grey) lines denote contours of constant $d_n(d_i^{2\text{-loop}})/d_n$, while red (dashed) lines are contours of constant $d_n(C_{bd})/d_n$, and finally green (dot-dashed) lines are contours of constant d_w/d_n . The thick solid black line delineates the experimental bound on $|d_n|$, and black dashed and dot-dashed lines represent constraints from direct searches for neutralinos and the Higgs.

eral very small, not exceeding 10% of the total d_n . Moreover, of particular relevance here, a scan over the parameter space of the CMSSM and NUHM reveals that the four-quark interactions and the Weinberg operator contribute at the 10% level at most. Both the Weinberg operator and the two loop contributions d_i^{2-loop} scale as $(\text{two-loop factor}) \times \tan \beta$ and therefore it is natural that they both contribute at a similar level. The contribution of four-fermion operators is dominated by C_{bd} and increases when m_0 is increased and/or m_A is lowered. Although outside the parameter regime included in the plots, it is worth noting that a factor of 3 increase in the maximum value of m_0 to around 3 TeV in Fig. 5c (at low m_A) would bring the C_{bd} contribution to a level comparable with $d_n(d_i, \tilde{d}_i)$.

We conclude that for all $m_0 < 1$ TeV the neutron EDM at large $\tan \beta$ can be reliably calculated in terms of the the EDMs and CEDMS of quarks. The hadronic uncertainties associated with the matrix elements of four-fermion and Weinberg operators, which we can only estimate within a factor of 3, do not significantly disrupt the predictions for d_n . This means that even at large $\tan \beta$ the calculation of d_n can provide meaningful constraints on specific combinations of the quark EDMs and CEDMs.

5.3 Mercury EDM

In many ways, the mercury EDM occupies an intermediate position between d_n and d_{Tl} . Results for the Hg EDM are shown in Fig. 6. Once again, the phenomenological and cosmological considerations are identical to those described for Fig. 4. In the CMSSM with $\theta_A \neq 0$ and $\theta_\mu = 0$, the current experimental constraint on d_{Hg} shows even greater sensitivity to m_0 than does d_n . On the other hand, the contribution of four-fermion operators to d_{Hg} is relatively less important than for d_{Tl} , but more important than for d_n . It is interesting to note that the contribution of C_S has a similar magnitude, but the opposite sign, to that of $C_{q_1 q_2}$, and over a large part of the parameter space these two effects tend to compensate each other. An exact cancellation would be an accident, as $C_{q_1 q_2}$ has considerable hadronic uncertainties associated with the calculation of the pion-nucleon CP-violating coupling and the Schiff moment. The contribution from C_P is negligible.

The effects of four-fermion operators become much more pronounced in the NUHM model. Fig.6c shows that for low m_A the mercury EDM receives contributions of up to 50% from C_S and $C_{q_1 q_2}$ (for the chosen parameters $d_{Hg}(C_S) \approx -d_{Hg}(C_{q_1 q_2})$ and only C_S is shown on the plot). These contributions drop quickly with increasing m_A and for $m_A > 250$ GeV do not exceed 10% of the total EDM. It is also important to note that for both the CMSSM and the NUHM the electron EDM remains subdominant for $\theta_A \neq 0$ and $\theta_\mu = 0$. This provides us with some confidence in the calculation of the mercury EDM at $\theta_A \neq 0$, $\theta_\mu = 0$ in the range $m_A > 250$ GeV and $m_0 < 1.5$ TeV where *both* d_e and four-fermion operators provide contributions of less than 10%. We conclude that in this part of the parameter space the mercury EDM is dominated by contributions from $(\tilde{d}_u - \tilde{d}_d)$.

This situation changes when we consider the case of $\theta_A = 0$, $\theta_\mu \neq 0$, shown in Fig. 6d. One can readily see that the electron EDM becomes important everywhere within the domain of parameter space included in the plot, and its inclusion leads to a significant

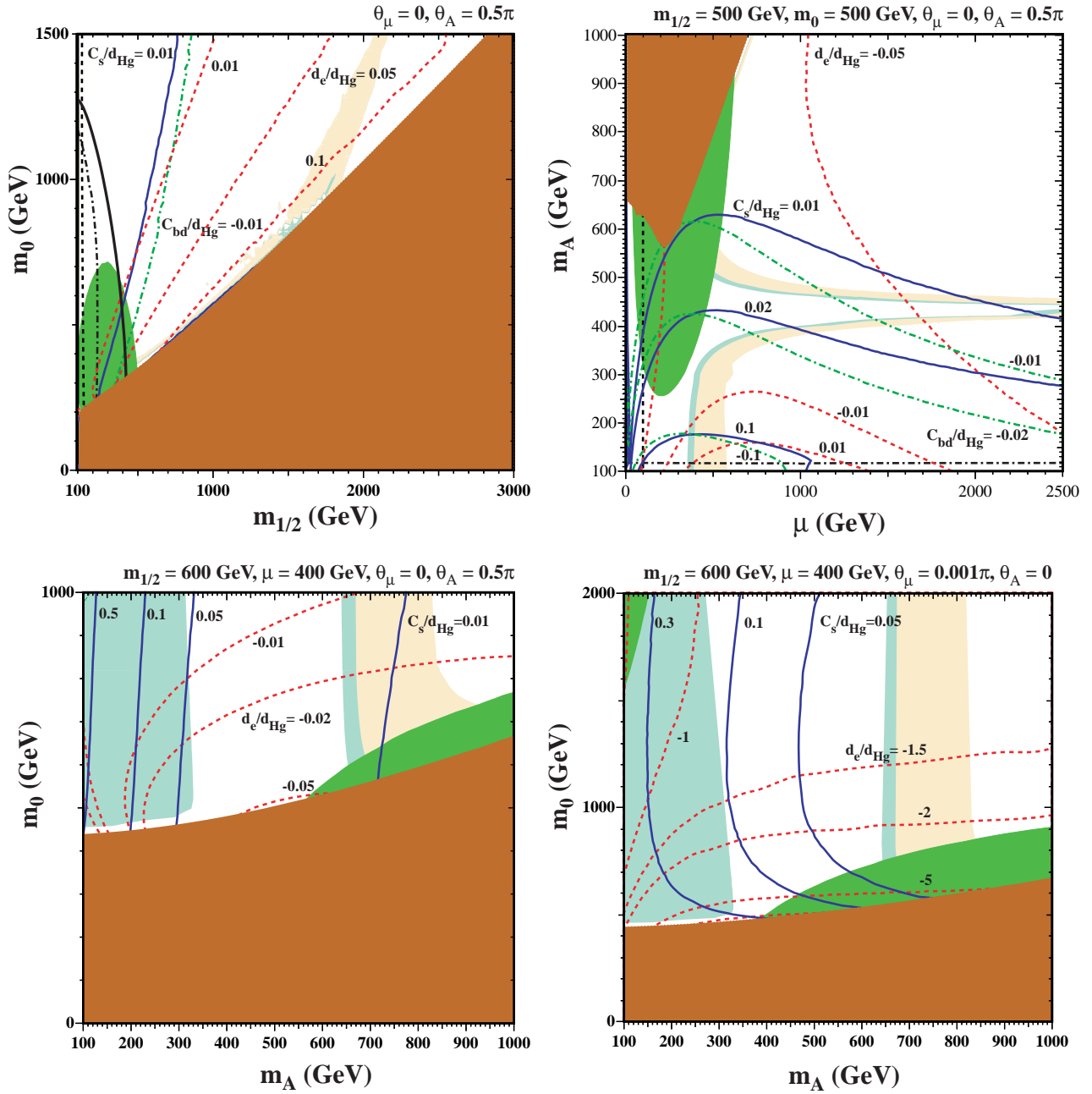


Figure 6: Contributions of the four-fermion operators and the electron EDM to the EDM of mercury as functions of the SUSY parameters. Blue (solid grey) lines denote contours of constant $d_{Hg}(C_S)/d_{Hg}$, while red (dashed) lines are the contours of constant $d_{Hg}(d_e)/d_{Hg}$ (indicated as d_e/d_{Hg}), and green (dot-dashed) lines are contours of constant $d_{Hg}(C_{bd})/d_{Hg}$ (indicated as C_{bd}/d_{Hg} on the plot). The thick solid black line denotes the experimental bound on $|d_{Hg}|$, while black dashed and dot-dashed lines represent constraints from direct searches for neutralinos and the Higgs.

reduction in the total mercury EDM. In practice, however, in this regime d_{TI} is dominated by d_e and, on taking the bound on d_{TI} into account, the effect of d_e on d_{Hg} will be suppressed. We note finally that, unlike the previous observables, at $\theta_A = 0$, $\theta_\mu \neq 0$ the mercury EDM also depends sensitively on C_S and the four-fermion contributions to the Schiff moment.

6 Conclusions

In this paper, we have presented the results of SUSY-EDM calculations in the large $\tan \beta$ regime. Large values of $\tan \beta$ are motivated by a variety of theoretical models and the SUSY Higgs searches at LEP also suggest that $\tan \beta \gtrsim 5$. Our main goal was to combine the existing one and two-loop calculations of the EDMs of the constituents (electrons, quarks, etc.) with the effects of four-fermion CP-odd interactions, the importance of which was recently emphasized in Ref. [26]. We concentrated on comparing the relative size of these contributions, while a more detailed analysis of the constraints on SUSY phases will appear elsewhere [68].

We have compiled the most accurate formulae to date to obtain the three observables: the EDMs of the neutron, mercury and thallium as functions of the Wilson coefficients, which in turn are expressed in terms of SUSY parameters. Mostly these are compilations of existing QCD/nuclear/atomic calculations, although in certain cases such as $d_n(C_{bd})$ and $d_{\text{Hg}}(C_{bd})$, new QCD estimates have been obtained. On the SUSY side, we have performed a complete calculation of 1-loop corrections to the quark and lepton masses in the large $\tan \beta$ regime, including the effects of SUSY CP-violating phases. These mass corrections (or rather their imaginary parts) determine the strength of the CP-violating Higgs-fermion interaction, the leading source for the CP-odd quark-quark and quark-electron interactions. At the subleading level, only the effects of scalar-pseudoscalar mixing were taken into account as these are important for low pseudoscalar masses m_A , although a large class of box diagrams can contribute as well. We also included the stau-loop contribution to the two-loop corrections to the EDMs, and recalculated the corresponding sign to firmly establish the pattern of interference between one- and two-loops.

The impact of the four-fermion operators is most striking for the thallium EDM. We observe that for low m_A and high m_0 the electron EDM is no longer dominant, and C_S provides as large a contribution (or possibly even larger) to d_{TI} as does d_e . A similar conclusion will apply to other paramagnetic species as well. This is an important point because it illustrates that in SUSY models with large $\tan \beta$, the EDM of a heavy paramagnetic atom or molecule cannot be entirely attributed to d_e . Should the next generation of paramagnetic EDM experiments [7, 8] detect a non-zero signal, only a combination of positive measurements with different atoms or molecules could unambiguously separate the two effects. It is also noteworthy that the total electron EDM is reduced due to destructive interference between the one- and two-loop contributions, particularly due to $\tilde{\tau}$ -loops.

In the C_S -dominated regime for d_{TI} , the main uncertainty in the theoretical calculation comes from the uncertainty of the strange quark scalar matrix element over the nucleon.

This translates into a 10% uncertainty when the EDM is induced by θ_A and 30 – 50% uncertainty for the θ_μ -induced EDM. The transition to dominance of C_S for $\theta_\mu \neq 0$ occurs at a very large mass scale for the superpartners, and in reality for $m_0 < 2$ TeV the contribution of $C_S(\theta_\mu)$ is always subdominant. Yet, in the case that the EDM is induced by θ_A , we find that the four-fermion operators can easily contribute as much as the electron EDM⁷. We also find that, in certain parts of the parameter space, the physical observable d_{Ti} is considerably smaller than the individual contributions.

In the case of the mercury EDM, there are a variety of different contributions that have to be taken into account. We find that at large $\tan \beta$ the contribution of C_S and other four-fermion operators may become important. From our analysis it is clear that the main problem with the interpretation of the mercury EDM at large $\tan \beta$ is that a rather large number of contributions appear with many of them having different hadronic/nuclear/atomic matrix elements. Therefore, a reliable calculation (i.e. better than 100% uncertainty) becomes problematic at large $\tan \beta$. This contrasts with low and moderate $\tan \beta$ where the EDM of mercury is usually dominated by the color EDMs of the light quarks, and the hadronic uncertainties are a less harmful overall factor. Nevertheless, for $\theta_\mu = 0$, $m_A \gtrsim 250$ GeV and $m_0 \lesssim 1.5$ TeV the effects of four-fermion operators and the electron EDM are subdominant and a meaningful estimate for d_{Hg} is possible.

We determined that the EDM of the neutron is the least susceptible observable, with the contributions of four fermion operators never exceeding 10% of the total EDM for $m_0 \lesssim 1$ TeV. On the other hand, for $\theta_A \neq 0$ the contribution of the Weinberg operator can be quite substantial. According to our estimates for the matrix elements, it is $\lesssim 10\%$ of the total EDM in much of the parameter space considered (if an NDA estimate of $d_n(w)$ is employed, this contribution is larger). Although subleading, we infer that at large $\tan \beta$ the calculation of the neutron EDM can be prone to uncertainties related to the matrix element of the Weinberg operator. It is also worth noting that the dominant, $\tan \beta$ -enhanced, contribution to the Weinberg operator comes from the color EDM of the b -quark.

Finally, we remark that low values of $m_A \lesssim 300$ GeV can be preferred by considerations of the cosmological neutralino abundance. This is related to the new annihilation channels due to Higgs exchange that open up when m_A is not excessively large. In that part of the parameter space the effects of four-fermion operators are very important, and therefore models that include both CP violation and neutralino dark matter should incorporate the effects of four-fermion interactions into the EDM constraints.

Acknowledgments

We would like to thank Y. Nir and Y. Santoso for helpful conversations. The work of DD and KAO was supported in part by DOE grant DE-FG02-94ER-40823. The work of MP

⁷We note also that additional $\tan \beta$ -enhanced contributions may arise through the electron EDM via two-loop renormalization group evolution of the gaugino masses. We will address these effects in more detail elsewhere [68].

was supported in part by NSERC of Canada and PPARC of the UK. AR would like to thank the FTPI at the University of Minnesota for generous hospitality while this work was completed.

Appendices

A Neutron EDM induced by four-fermion operators

As discussed in Section 4, the direct QCD sum-rule analysis for the neutron EDM becomes problematic for sources of dimension six, due in part to the presence of unknown condensates. For the contribution of the Weinberg operator, one can nonetheless obtain a useful estimate [60] by relating d_n to the neutron anomalous magnetic moment, μ_n , by a chiral rotation of the nucleon wavefunction. For similar reasons, we will adopt the same approach here in estimating the contribution of the four fermion sources to the neutron EDM.

To proceed, it is convenient to first introduce a redefined set of Wilson coefficients, so that

$$\delta\mathcal{L} = \tilde{C}_{bd}(m_b)m_b\bar{b}b\bar{d}i\gamma_5d + \tilde{C}_{db}(m_b)m_b\bar{d}d\bar{b}i\gamma_5b, \quad (\text{A.65})$$

at the b -quark mass scale, where $\tilde{C} = C/m_b$. Below this scale, the b -quarks can be integrated out leading to dimension-7 quark-gluon operators. Making use of the standard low energy theorems we obtain

$$\delta\mathcal{L} = -\frac{\alpha_s(\mu)\tilde{C}_{bd}(\mu)}{12\pi}\bar{d}i\gamma_5dGG - \frac{\alpha_s(\mu)\tilde{C}_{db}(\mu)}{16\pi}\bar{d}dG\tilde{G}. \quad (\text{A.66})$$

The evolution of the coefficients to the hadronic scale $\mu \sim 1$ GeV requires knowledge of the anomalous dimensions of these dimension-7 operators. Since (with hindsight), the overall contribution of these operators is small, we will approximate this by the anomalous dimension of $\bar{q}q$, recalling that $\alpha_s GG$ is RG-invariant. Thus, we run \tilde{C}_{bd} and \tilde{C}_{db} to $\mu \sim 1$ GeV, using $\gamma_{\alpha_s\bar{q}qGG} \sim 4/9$.

To gain some intuition about the dependence of d_n on $\tilde{C}(\mu)$, we first utilize “naive dimensional analysis” [54, 55]. The quark-gluon operators are of dimension-7, so the reduced coupling is $M^3/(4\pi)^2$ with $M \sim 4\pi f_\pi$. The corresponding estimate for d_n is given by e/M multiplied by the reduced coupling of the source, and so we find

$$|d_n(\text{NDA})| \sim e 2.1 \times 10^{-3} \text{ GeV}^2 \left(\tilde{C}_{bd}(\mu) + 0.75 \tilde{C}_{db}(\mu) \right), \quad (\text{A.67})$$

on using the usual matching condition $\alpha_s = 4\pi$, i.e. at a very low (apparent) scale. As it turns out, our final estimate is quite close to this, assuming we choose the matching scale not too far from 1 GeV.

We now turn to a sum-rule analysis. As alluded to above, a direct calculation appears intractable due to the presence of unknown condensates. Therefore, we will pursue instead

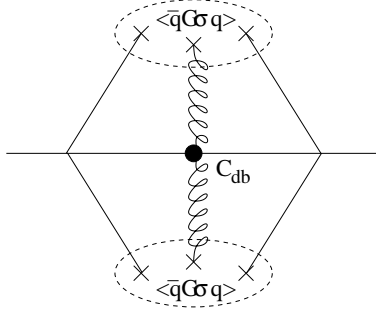


Figure 7: The leading contribution to the γ_5 structure induced by the CP-odd source.

an indirect method first considered by Bigi and Uraltsev [76], and used recently within QCD sum-rules to estimate d_n induced by the Weinberg operator $GG\tilde{G}$. One considers the γ_5 -rotation of the nucleon wavefunction induced by $\delta\mathcal{L}$, leading to an estimate for d_n in terms of the corresponding rotation of the anomalous magnetic moment μ_n :

$$d_n \sim \mu_n \frac{\langle N|\delta\mathcal{L}|N\rangle}{m_n \bar{N} i\gamma_5 N}. \quad (\text{A.68})$$

In the present context, we require the ratio of the leading contributions to the structures **1** and $i\gamma_5$ in the mass sum-rule correlator. We have

$$\int d^4x e^{ip\cdot x} \langle \eta_n(0) \bar{\eta}_n(x) \rangle = \frac{1}{16\pi^2} \langle \bar{q}q \rangle \left[p^2 \ln(-p^2) \mathbf{1} + f_\delta(p^2) i\gamma_5 \right], \quad (\text{A.69})$$

where η_n is the neutron current, which for the mass sum-rule we take at the “Ioffe point” [77], f_δ is the contribution induced by the CP-odd source $\delta\mathcal{L}$ that is to be determined, and we have retained only the leading order contribution to the structure **1**.

Fortunately, in this case the leading contribution enters in a tractable form without the need for additional perturbative vertices – i.e. the gluon structure of the source $\delta\mathcal{L}$ can be extracted at the nonperturbative level. The relevant class of diagrams is exhibited in Fig. 7. Using standard methods, we calculate the quark propagators in the background of the two sources in $\delta\mathcal{L}$ making use of the known quark-gluon condensate⁸:

$$\langle \bar{q}g_s(G\sigma)q \rangle = \tilde{m}_0^2 |\langle \bar{q}q \rangle| \approx 0.8 \text{GeV}^2 \langle \bar{q}q \rangle. \quad (\text{A.70})$$

One then obtains,

$$f_\delta(p^2) = -\frac{\tilde{m}_0^4}{6p^2} \langle \bar{q}q \rangle \left(\tilde{C}_{bd} + 0.75 \tilde{C}_{db} \right), \quad (\text{A.71})$$

and we proceed by performing a Borel transform and comparing the two terms in (A.69) at the neutron mass scale in terms of the Borel parameter M . This fixes the ratio of the

⁸We have introduced a tilde atop m_0 in order to distinguish this QCD condensate from the mass of the SUSY scalars.

two structures in (A.69) which is the quantity that enters the estimate (A.68), leading to the result,

$$|d_n| \sim |\mu_n| \frac{\tilde{m}_0^4}{6M} \langle \bar{q}q \rangle (\tilde{C}_{bd} + 0.75 \tilde{C}_{db}) \sim e 2.6 \times 10^{-3} \text{GeV}^2 (\tilde{C}_{bd} + 0.75 \tilde{C}_{db}), \quad (\text{A.72})$$

which necessarily comes with a precision estimate not better than $\mathcal{O}(100\%)$. On re-expressing this result in terms of C_{bd} and C_{db} , we obtain the result quoted in (4.57).

Finally, for completeness, we note that the operators C_{dd} , C_{ds} , C_{sd} and C_{ss} can be generated via $H - A$ mixing. Their contribution to the neutron EDM can be estimated as [9, 35]:

$$\frac{d_n(C_{dd})}{C_{dd}} \sim \frac{d_n(C_{sd})}{C_{sd}} \sim 2 \times 10^{-2} \text{GeV}, \quad \frac{d_n(C_{ds})}{C_{ds}} \sim \frac{d_n(C_{ss})}{C_{ss}} \sim 2 \times 10^{-3} \text{GeV}. \quad (\text{A.73})$$

B Mercury EDM induced by four-fermion operators

The main source for the Schiff moment of the mercury nucleus arises through a pion-exchange contribution with CP violation in the pion-nucleon vertex,

$$\mathcal{L}_{\pi NN} = \bar{g}_{\pi NN}^{(0)} \bar{N} \tau^a N \pi^a + \bar{g}_{\pi NN}^{(1)} \bar{N} N \pi^0 + \bar{g}_{\pi NN}^{(2)} (\bar{N} \tau^a N \pi^a - 3 \bar{N} \tau^3 N \pi^0), \quad (\text{B.74})$$

of which the contribution of $\bar{g}_{\pi NN}^{(1)}$ is the most important [67, 66]. We recall here that the main technical difficulty in the derivation of this coupling, as induced by color EDM operators, is the existence of two compensating diagrams. The direct chiral commutator $[J_{05}, \bar{q}(G\sigma)\gamma_5 q]$ tends to cancel against a pion re-scattering diagram (see Ref. [67] for details). The resulting expression for $\bar{g}_{\pi NN}^{(1)}$ is given by the following linear combination of nucleon matrix elements for $\bar{q}g_s(G\sigma)q$ and $\bar{q}q$:

$$\frac{\tilde{d}_u - \tilde{d}_d}{4f_\pi} \langle N | \bar{u}g_s(G\sigma)u + \bar{d}g_s(G\sigma)d - \tilde{m}_0^2(\bar{u}u + \bar{d}d) | N \rangle. \quad (\text{B.75})$$

This vanishes if $\langle N | \bar{q}g_s(G\sigma)q | N \rangle = \tilde{m}_0^2 \langle N | \bar{q}q | N \rangle$, a relation that holds in the vacuum factorization approximation. Thus, in order to obtain a non-zero result, one has to go beyond the factorization approximation. A full QCD sum-rule analysis [67] produces a preferred range for this coupling with the “best” value given by

$$\bar{g}_{\pi NN}^{(1)} = 2 \times 10^{14} (\tilde{d}_u - \tilde{d}_d) \text{ cm}^{-1}. \quad (\text{B.76})$$

Combined with the relevant nuclear, $S(\bar{g}_{\pi NN}^{(1)})$, and atomic, $d_{\text{Hg}}(S)$, pieces of the calculation, this expression enters the first line of Eq. (4.61).

After this brief review of the color EDM contributions to $\bar{g}_{\pi NN}^{(1)}$, for large $\tan \beta$ we also need to generalize this derivation to include $\bar{g}_{\pi NN}^{(1)}(C_{q_1 q_2})$. Both diagrams, the direct chiral commutator and the pion re-scattering diagram, are present in this case as well. Luckily,

in contrast with the case of CEDM sources, vacuum factorization does now produce a non-zero result. Combining these two diagrams, we find a contribution that corresponds to the *direct factorization* of the pseudoscalar bilinear $\bar{q}i\gamma_5 q$ via the chiral commutator with the pion. The final expression for $\bar{g}_{\pi NN}^{(1)}$ takes the form,

$$\begin{aligned}\bar{g}_{\pi NN}^{(1)} &= \frac{\langle \bar{q}q \rangle}{2f_\pi} \langle N | C_{dd} \bar{d}d + C_{sd} \bar{s}s + C_{bd} \bar{b}b | N \rangle \\ &= -8 \times 10^{-2} \text{GeV}^2 \left(\frac{0.5C_{dd}}{m_d} + 3.3\kappa \frac{C_{sd}}{m_s} + \frac{C_{bd}}{m_b} (1 - 0.25\kappa) \right).\end{aligned}\quad (\text{B.77})$$

Note that within the factorization approximation C_{db} , C_{ds} , C_{ss} and C_{bb} do not contribute to $\bar{g}_{\pi NN}^{(1)}$. The final expression (B.77) depends on the same matrix element of $\bar{s}s$ over the nucleon as previously encountered in the calculation of C_S , and parametrized by κ .

References

- [1] P. G. Harris *et al.*, Phys. Rev. Lett. **82** (1999) 904.
- [2] B. C. Regan *et al.*, Phys. Rev. Lett. **88** (2002) 071805.
- [3] M. V. Romalis, W. C. Griffith and E. N. Fortson, Phys. Rev. Lett. **86** (2001) 2505.
- [4] D. Cho, K. Sangster, E.A. Hinds, Phys. Rev. Lett. **63** (1989) 2559.
- [5] M. A. Rosenberry and T. E. Chupp, Phys. Rev. Lett. **86** (2001) 22.
- [6] S.A. Murthy *et al.*, Phys. Rev. Lett. **63** (1989) 965.
- [7] J. Hudson, B. E. Sauer, M. R. Tarbutt, and E. A. Hinds, Phys. Rev. Lett. **89** (2002) 023003.
- [8] D. DeMille *et al.*, Phys. Rev. A **61** (2000) 052507.
- [9] I.B. Khriplovich and S.K. Lamoreaux, *"CP Violation Without Strangeness"*, Springer, 1997.
- [10] LEP Higgs Working Group for Higgs boson searches, OPAL Collaboration, ALEPH Collaboration, DELPHI Collaboration and L3 Collaboration, Phys. Lett. B **565** (2003) 61 [arXiv:hep-ex/0306033]. *Searches for the neutral Higgs bosons of the MSSM: Preliminary combined results using LEP data collected at energies up to 209 GeV*, LHWG-NOTE-2001-04, ALEPH-2001-057, DELPHI-2001-114, L3-NOTE-2700, OPAL-TN-699, arXiv:hep-ex/0107030; LHWG Note/2002-01, http://lephiggs.web.cern.ch/LEPHIGGS/papers/July2002_SM/index.html; J. R. Ellis, G. Ganis, D. V. Nanopoulos and K. A. Olive, Phys. Lett. B **502** (2001) 171; See also H. E. Haber, "Higgs theory and phenomenology in the standard model and MSSM," arXiv:hep-ph/0212136.

- [11] For some recent papers see: T. Blazek, R. Dermisek and S. Raby, Phys. Rev. Lett. **88** (2002) 111804; U. Chattopadhyay, A. Corsetti and P. Nath, Phys. Rev. D **66** (2002) 035003; K. Tobe and J. D. Wells, Nucl. Phys. B **663** (2003) 123; D. Auto, H. Baer, C. Balazs, A. Belyaev, J. Ferrandis and X. Tata, JHEP **0306**, 023 (2003).
- [12] J. R. Ellis, S. Ferrara and D. V. Nanopoulos, Phys. Lett. B **114** (1982) 231; W. Buchmuller and D. Wyler, Phys. Lett. B **121** (1983) 321; J. Polchinski and M. B. Wise, Phys. Lett. B **125** (1983) 393; M. Dugan, B. Grinstein and L. Hall, Nucl. Phys. **B255** (1985) 413.
- [13] T. Falk and K. A. Olive, Phys. Lett. B **375** (1996) 196; T. Falk and K.A. Olive, Phys. Lett. **B439** (1998) 71.
- [14] T. Ibrahim and P. Nath, Phys. Lett. B **418** (1998) 98; Phys. Rev. D **57** (1998) 478; [Erratum-ibid. D **58** (1998) 019901]; Phys. Rev. D **58** (1998) 111301.
- [15] M. Brhlik, G. J. Good and G. L. Kane, Phys. Rev. D **59** (1999) 115004; M. Brhlik, L. L. Everett, G. L. Kane and J. Lykken, Phys. Rev. Lett. **83** (1999) 2124; A. Bartl, T. Gajdosik, W. Porod, P. Stockinger and H. Stremnitzer, Phys. Rev. D **60** (1999) 073003; S. Pokorski, J. Rosiek and C. A. Savoy, Nucl. Phys. B **570**, (2000) 81.
- [16] T. Falk, K.A. Olive, M. Pospelov and R. Roiban, Nucl. Phys. B **560** (1999) 3.
- [17] V. D. Barger, T. Falk, T. Han, J. Jiang, T. Li and T. Plehn, Phys. Rev. D **64** (2001) 056007.
- [18] S. Abel, S. Khalil and O. Lebedev, Phys. Rev. Lett. **86** (2001) 5850; Nucl. Phys. B **606** (2001) 151.
- [19] S. Abel, S. Khalil and O. Lebedev, Phys. Rev. Lett. **89** (2002) 121601.
- [20] O. Lebedev and S. Morris, JHEP **0208** (2002) 007.
- [21] P. Nath, Phys. Rev. Lett. **66** (1991) 2565; Y. Kizukuri and N. Oshimo, Phys. Rev. D **45** (1992) 1806; **D46** (1992) 3025; A. G. Cohen, D. B. Kaplan and A. E. Nelson, Phys. Lett. B **388** (1996) 588.
- [22] J. Kubo and H. Terao, Phys. Rev. D **66** (2002) 116003.
- [23] R. N. Mohapatra and G. Senjanovic, Phys. Lett. B **79** (1978) 283; S. M. Barr, Phys. Rev. Lett. **53** (1984) 329; A. E. Nelson, Phys. Lett. B **136** (1984) 387.
- [24] S. Dimopoulos and S. Thomas, Nucl. Phys. B **465** (1996) 23; R. Kuchimanchi, Phys. Rev. Lett. **76** (1996) 3486; R. N. Mohapatra and A. Rasin, Phys. Rev. Lett. **76** (1996) 3490; M. E. Pospelov, Phys. Lett. B **391** (1997) 324; G. Hiller and M. Schmaltz, Phys. Lett. B **514** (2001) 263.
- [25] S. M. Barr, Phys. Rev. Lett. **68** (1992) 1822; Phys. Rev. D **47** (1993) 2025.

- [26] O. Lebedev and M. Pospelov, Phys. Rev. Lett. **89** (2002) 101801.
- [27] J. R. Ellis, T. Falk, G. Ganis, K. A. Olive and M. Srednicki, Phys. Lett. B **510**, 236 (2001); M. Battaglia *et al.*, Eur. Phys. J. **C22** (2001) 535; J. R. Ellis, K. A. Olive and Y. Santoso, New J. Phys. **4** (2002) 32.
- [28] Some additional recent papers include: A. B. Lahanas, D. V. Nanopoulos and V. C. Spanos, Phys. Lett. B **518** (2001) 94; V. D. Barger and C. Kao, Phys. Lett. B **518** (2001) 117; L. Roszkowski, R. Ruiz de Austri and T. Nihei, JHEP **0108** (2001) 024; A. Djouadi, M. Drees and J. L. Kneur, JHEP **0108** (2001) 055; U. Chattopadhyay, A. Corsetti and P. Nath, Phys. Rev. D **66** (2002) 035003; H. Baer, C. Balazs, A. Belyaev, J. K. Mizukoshi, X. Tata and Y. Wang, JHEP **0207** (2002) 050.
- [29] V. Berezinsky, A. Bottino, J. R. Ellis, N. Fornengo, G. Mignola and S. Scopel, Astropart. Phys. **5** (1996) 1; P. Nath and R. Arnowitt, Phys. Rev. D **56** (1997) 2820; A. Bottino, F. Donato, N. Fornengo and S. Scopel, Phys. Rev. D **59** (1999) 095004; Phys. Rev. D **63**, 125003 (2001); R. Arnowitt, B. Dutta and Y. Santoso, Nucl. Phys. B **606** (2001) 59; V. Bertin, E. Nezri and J. Orloff, JHEP **0302** (2003) 046.
- [30] J. R. Ellis, K. A. Olive and Y. Santoso, Phys. Lett. B **539** (2002) 107; J. R. Ellis, T. Falk, K. A. Olive and Y. Santoso, Nucl. Phys. B **652** (2003) 259.
- [31] O. Lebedev, Phys. Rev. D **67** (2003) 015013.
- [32] R. D. Peccei and H. R. Quinn, Phys. Rev. Lett. **38** (1977) 1440.
- [33] V. M. Khatsimovsky, I. B. Khriplovich and A. S. Yelkhovsky, Annals Phys. **186** (1988) 1.
- [34] X. G. He and B. McKellar, Phys. Lett. B **390** (1997) 318.
- [35] C. Hamzaoui and M. Pospelov, Phys. Rev. D **65** (2002) 056002.
- [36] R. Hempfling, Phys. Rev. D **49** (1994) 6168; L. J. Hall, R. Rattazzi and U. Sarid, Phys. Rev. D **50** (1994) 7048; T. Blazek, S. Raby and S. Pokorski, Phys. Rev. D **52** (1995) 4151; C. Hamzaoui, M. Pospelov and M. Toharia, Phys. Rev. D **59** (1999) 095005; K. S. Babu and C. F. Kolda, Phys. Rev. Lett. **84** (2000) 228.
- [37] A. Pilaftsis, Nucl. Phys. B **644** (2002) 263.
- [38] H. E. Haber and G. L. Kane, Phys. Rept. **117** (1985) 75; J. F. Gunion and H. E. Haber, Nucl. Phys. B **272** (1986) 1.
- [39] G. Passarino and M. J. Veltman, Nucl. Phys. B **160** (1979) 151.
- [40] O. Lebedev and W. Loinaz, Phys. Rev. D **65** (2002) 033005.
- [41] T. Blazek, S. Raby and S. Pokorski, in Ref.[36].

- [42] D. M. Pierce, J. A. Bagger, K. T. Matchev and R. J. Zhang, Nucl. Phys. B **491** (1997) 3.
- [43] T. Ibrahim and P. Nath, Phys. Rev. D **67** (2003) 095003 [Erratum-ibid. D **68** (2003) 019901]; arXiv:hep-ph/0311242.
- [44] A. Pilaftsis, Phys. Lett. B **435** (1998) 88; D. A. Demir, Phys. Rev. D **60** (1999) 055006; A. Pilaftsis and C. E. M. Wagner, Nucl. Phys. B **553** (1999) 3.
- [45] Z. W. Liu and H. P. Kelly, Phys. Rev. A **45** (1992) R4210.
- [46] A.-M. Martensson-Pendrill, *Methods in Computational Chemistry, Volume 5: Atomic, Molecular Properties*, ed. S. Wilson (Plenum Press, New York 1992).
- [47] E. Lindroth, A.-M. Martensson-Pendrill, Europhys. Lett. **15** (1991) 155.
- [48] J. S. M. Ginges and V. V. Flambaum, arXiv:physics/0309054.
- [49] D. Chang, W. Y. Keung and A. Pilaftsis, Phys. Rev. Lett. **82** (1999) 900 [Erratum-ibid. **83** (1999) 3972].
- [50] A. Pilaftsis, Phys. Lett. B **471** (1999) 174.
- [51] D. Chang, W. F. Chang and W. Y. Keung, Phys. Rev. D **66** (2002) 116008.
- [52] M. A. Shifman, A. I. Vainshtein and V. I. Zakharov, Phys. Lett. B **78** (1978) 443.
- [53] H.-Y. Cheng, Phys. Lett. **B219** (1989) 347; J. Gasser, H. Leutwyler, and M. E. Sainio, Phys. Lett. **B253** (1991) 252; H. Leutwyler, hep-ph/9609465; B. Borasoy and U. G. Meissner, Annals Phys. **254** (1997) 192; M. Knecht, PiN Newslett. **15** (1999) 108 [arXiv:hep-ph/9912443].
- [54] A. Manohar and H. Georgi, Nucl. Phys. B **234** (1984) 189.
- [55] S. Weinberg, Phys. Rev. Lett. **63** (1989) 2333.
- [56] R. J. Crewther, P. Di Vecchia, G. Veneziano and E. Witten, Phys. Lett. B **88** (1979) 123 [Erratum-ibid. B **91** (1980) 487].
- [57] V. M. Khatsymovsky and I. B. Khriplovich, Phys. Lett. B **296** (1992) 219.
- [58] S. Aoki *et al.*, Phys. Rev. **D56** (1997) 433.
- [59] M. Pospelov and A. Ritz, Phys. Rev. Lett. **83** (1999) 2526; Nucl. Phys. B **573** (2000) 177; Phys. Rev. D **63** (2001) 073015.
- [60] D. A. Demir, M. Pospelov and A. Ritz, Phys. Rev. D **67** (2003) 015007.
- [61] D. Chang, T. W. Kephart, W. Y. Keung and T. C. Yuan, Phys. Rev. Lett. **68** (1992) 439.

- [62] R. Arnowitt, J.L. Lopez and D. V. Nanopoulos, Phys. Rev. D **42** (1990) 2423.
- [63] J. Dai, H. Dykstra, R. G. Leigh, S. Paban and D. Dicus, Phys. Lett. B **237** (1990) 216 [Erratum-ibid. B **242** (1990) 547].
- [64] L.I. Schiff, Phys. Rev. **132** (1963) 2194.
- [65] V. A. Dzuba, V. V. Flambaum, J. S. Ginges and M. G. Kozlov, Phys. Rev. A **66** (2002) 012111
- [66] V. F. Dmitriev and R. A. Sen'kov, arXiv:nucl-th/0304048.
- [67] M. Pospelov, Phys. Lett. B **530** (2002) 123.
- [68] D. Demir, O. Lebedev, K. Olive, M. Pospelov and A. Ritz, in preparation.
- [69] Joint LEP 2 Supersymmetry Working Group, *Combined LEP Chargino Results, up to 208 GeV*, http://lepsusy.web.cern.ch/lepsusy/www/inos_moriond01/charginos_pub.html.
- [70] S. Heinemeyer, W. Hollik and G. Weiglein, Comput. Phys. Commun. **124** (2000) 76; S. Heinemeyer, W. Hollik and G. Weiglein, Eur. Phys. J. C **9** (1999) 343.
- [71] M.S. Alam et al., [CLEO Collaboration], Phys. Rev. Lett. **74** (1995) 2885 as updated in S. Ahmed et al., CLEO CONF 99-10; BELLE Collaboration, BELLE-CONF-0003, contribution to the 30th International conference on High-Energy Physics, Osaka, 2000. See also K. Abe *et al.*, [Belle Collaboration], [arXiv:hep-ex/0107065]; L. Lista [BaBar Collaboration], [arXiv:hep-ex/0110010]; C. Degrassi, P. Gambino and G. F. Giudice, JHEP **0012** (2000) 009; M. Carena, D. Garcia, U. Nierste and C. E. Wagner, Phys. Lett. B **499** (2001) 141; D. A. Demir and K. A. Olive, Phys. Rev. D **65** (2002) 034007; T. Hurth, arXiv:hep-ph/0106050; F. Borzumati, C. Greub and Y. Yamada, arXiv:hep-ph/0311151.
- [72] C. L. Bennett *et al.*, Astrophys. J. Suppl. **148** (2003) 1; D. N. Spergel *et al.*, Astrophys. J. Suppl. **148** (2003) 175.
- [73] J. R. Ellis, K. A. Olive, Y. Santoso and V. C. Spanos, Phys. Lett. B **565** (2003) 176; M. Battaglia, A. De Roeck, J. R. Ellis, F. Gianotti, K. A. Olive and L. Pape, arXiv:hep-ph/0306219. H. Baer and C. Balazs, JCAP **0305** (2003) 006; A. B. Lahanas and D. V. Nanopoulos, Phys. Lett. B **568** (2003) 55; U. Chattopadhyay, A. Corsetti and P. Nath, Phys. Rev. D **68** (2003) 035005.
- [74] J. R. Ellis, A. Ferstl, K. A. Olive and Y. Santoso, Phys. Rev. D **67** (2003) 123502.
- [75] J. Ellis, K. A. Olive, Y. Santoso and V. C. Spanos, arXiv:hep-ph/0310356.
- [76] I. I. Bigi and N. G. Uraltsev, Nucl. Phys. B **353**, 321 (1991).
- [77] B. L. Ioffe, Z. Phys. C **18**, 67 (1983).